Unified interpretation of Hund's first and second rules for 2*p* and 3*p* atoms

Takayuki Oyamada,[1,a)] Kenta Hongo,[2,b)] Yoshiyuki Kawazoe,[3] and Hiroshi Yasuhara[3]
[1]*Department of Chemistry, Graduate School of Science, Tohoku University, 6-3 Aoba, Aramaki, Aoba-ku, Sendai 980-8578, Japan*
[2]*Department of Chemistry and Chemical Biology, Harvard University, 12 Oxford Street, Cambridge, Massachusetts 02138, USA*
[3]*Institute for Materials Research, Tohoku University, 2-1-1 Katahira, Aoba-ku, Sendai 980-8577, Japan*

(Received 22 April 2010; accepted 17 August 2010; published online 29 October 2010)

A unified interpretation of Hund's first and second rules for 2*p* (C, N, O) and 3*p* (Si, P, S) atoms is given by Hartree–Fock (HF) and multiconfiguration Hartree–Fock (MCHF) methods. Both methods exactly satisfy the virial theorem, in principle, which enables one to analyze individual components of the total energy $E(=T+V_{en}+V_{ee})$, where T, V_{en}, and V_{ee} are the kinetic, the electron-nucleus attraction, and the electron-electron repulsion energies, respectively. The correct interpretation for each of the two rules can only be achieved under the condition of the virial theorem $2T+V=0$ by investigating how V_{en} and V_{ee} interplay to attain the lower total potential energy $V(=V_{en}+V_{ee})$. The stabilization of the more stable states for all the 2*p* and 3*p* atoms is ascribed to a greater V_{en} that is caused by contraction of the valence orbitals accompanied with slight expansion of the core orbitals. The contraction of the valence orbitals for the two rules is a consequence of reducing the Hartree screening of the nucleus at short interelectronic distances. The *reduced screening* in the first rule is due to a greater amount of Fermi hole contributions in the state with the highest total spin-angular momentum *S*. The reduced screening in the second rule is due to the fact that two valence electrons are more likely to be on opposite sides of the nucleus in the state with the highest total orbital-angular momentum *L*. For each of the two rules, the inclusion of correlation does not qualitatively change the HF interpretation, but HF overestimates the energy difference $|\Delta E|$ between two levels being compared. The magnitude of the correlation energy is significantly larger for the lower *L* states than for the higher *L* states since two valence electrons in the lower *L* states are less likely to be on opposite sides of the nucleus. The MCHF evaluation of $|\Delta E|$ is in excellent agreement with experiment. The present HF and MCHF calculations demonstrate the above statements that were originally given by Katriel [Theor. Chem. Acta **23**, 309 (1972); **26**, 163 (1972)]. We have, for the first time, analyzed the correlation-induced changes in the radial density distribution for the excited *LS* terms of the 2*p* and 3*p* atoms as well as for the ground *LS* term. © *2010 American Institute of Physics*. [doi:10.1063/1.3488099]

I. INTRODUCTION

In a series of our previous studies,[1–4] we have interpreted Hund's first rule (i.e., spin-multiplicity rule) for the ground and lowest excited states of 2*p* (carbon, nitrogen, and oxygen) and 3*p* (silicon, phosphorus, and sulfur) atoms by quantum Monte Carlo (QMC) methods. Our previous QMC calculations have systematically given the correct interpretation of Hund's first rule for those atoms, taking due account of correlation. They have, however, overestimated the energy difference $|\Delta E|$ between the ground and the lowest excited states as compared with the experiment. The overestimate above is attributed to our rather crude description of excited states that is unable to discriminate between excited states with a different total orbital-angular momentum *L*. The nodal part of QMC trial wavefunction was constructed from a single Slater determinant. Generally, such a treatment is appropriate for most eigenfunctions of the total spin-angular momentum *S* but often not for eigenfunctions of *L*. To appropriately describe *LS* terms of the open-shell atoms, it is necessary to construct the wavefunction from an appropriate linear combination of few Slater determinants especially for excited states.[5]

In this study, we give a unified interpretation of Hund's first and second rules for the 2*p* and 3*p* atoms by numerical Hartree–Fock (HF) and multiconfiguration Hartree–Fock (MCHF) methods. MCHF takes due account of correlation, which is beyond the scope of HF. Both methods correctly specify *LS* terms of the atoms that are represented as ^{2S+1}L in the Russell–Saunders notation.

The present MCHF is sufficiently accurate to clarify the role of correlation in a unified interpretation of Hund's first and second rules. HF overestimates $|\Delta E|$ between the two stationary states being compared in each of Hund's first and second rules. $|\Delta E|$ evaluated by MCHF is in excellent agreement with the experiment. The correct interpretation of Hund's first and second rules can only be achieved under the condition of the virial theorem $2T+V=0$ by investigating

[a)]Author to whom correspondence should be addressed. Electronic mail: oyamadat@imr.edu.
[b)]Japan Society for the Promotion of Science Postdoctoral Fellow for Research Abroad.

how V_{en} and V_{ee} interplay to attain the lower total potential energy $V(=V_{en}+V_{ee})$,[6,7] where T, V_{en}, and V_{ee} are the kinetic, the electron-nucleus attraction, and the electron-electron repulsion energies, respectively. Both of the two methods satisfy the virial theorem, which enables one to make a detailed analysis of the individual energy components of the total energy E, the correlation energy E^{corr}, and the energy difference ΔE.

The present study deals with six different types of LS terms arising from the ground configuration of the $2p$ and $3p$ atoms: three different types of LS terms, i.e., the ^3P, ^1D, and ^1S terms arise from the $ns^2np^2(n=2,3)$ configuration of the C and Si atoms and the $ns^2np^4(n=2,3)$ configuration of the O and S atoms. The remaining three different types of LS terms, i.e., the ^4S, ^2D, and ^2P terms arise from the $ns^2np^3(n=2,3)$ configuration of the N and P atoms. The first rule applies to a comparison of the ground and the first-excited LS terms and the second rule to a comparison of the first- and the second-excited LS terms.

Just before the advent of quantum mechanics (1925), Hund found useful empirical rules to determine the ground state from an analysis of atomic spectra.[8] These empirical rules have been generalized to the well-known formula as follows.

First rule. Among the states arising from a given electronic configuration, the lowest is the one having the highest total spin angular momentum S.

Second rule. Among the states of the same configuration with the same S value, the lowest is the one having the highest total orbital angular momentum L.

In short, both the first and second rules imply that the stationary state with the largest possible total spin- and orbital-angular momentum is the most stable. Hund's first rule has traditionally been explained in terms of a reduction in the electron-electron repulsion energy V_{ee} due to the Pauli exclusion principle[9] in almost all textbooks, except for a few modern ones.[10–12] On the other hand, only a few textbooks have attempted to explain the second rule. These explanations appeal to a reduction in V_{ee} due to another mechanism: the larger L value means that two electrons are more likely to go around the nucleus in the same direction, repelling each other less frequently, and hence the electron-electron repulsion is reduced in the larger L state.[5]

The traditional interpretation of Hund's rules is, in fact, significantly different from the first-order perturbational interpretation, although the two interpretations give the same E and V_{ee}. The so-called traditional interpretation relies on the assumption that the different LS terms arising from the same electronic configuration could have the same set of orbitals. As a result, it gives the same T and V_{en} for the two LS terms being compared, and hence the virial theorem is not satisfied. On the other hand, the first-order perturbative wavefunction satisfies the virial theorem within the same order,[13,14] so far as it is constructed from a complete set of unperturbed wavefunctions $\{\psi_n^{(0)}\}$. Killingbeck[13] generally proved that the magnitude of the first-order correction to V_{en} and T is the same as that of the first-order correction to E, i.e., $V_{en}^{(1)}=-T^{(1)}=E^{(1)}=V_{ee}^{(1)}=\langle\psi_n^{(0)}|\hat{V}_{ee}|\psi_n^{(0)}\rangle$, and hence the first-order perturbational virial theorem $2T^{(1)}+V_{en}^{(1)}+V_{ee}^{(1)}=0$ holds. Katriel and Pauncz[7] applied these relations to the first-order perturbational interpretation of Hund's rules. In this treatment, both V_{en} and V_{ee} are lowered by the same amount in the more stable state. Thus, the two interpretations are different in physical contents, although the two give the same value of E and V_{ee} due to the complete cancellation between $V_{en}^{(1)}$ and $T^{(1)}$.

However, both the traditional and the first-order perturbational interpretations of Hund's first and second rules are incorrect since the two interpretations give the lower V_{ee} in the more stable state. In fact, V_{ee} is higher in the more stable state, as has been confirmed from the exact variational calculation for the excited states of the helium atom.[15,16] Correctly, both the two rules are ascribed to a greater V_{en} due to contraction of valence p orbitals toward the nucleus in the more stable state. At the same time, the valence p orbitals penetrate into the immediate vicinity of the nucleus to give an extra screening, which causes a slight but significant expansion of the core s orbitals. A combination of contraction of the valence p orbitals and expansion of the core s orbitals increases V_{ee} in the more stable states,[6,7] in contrast to the traditional explanation.

The virial theorem is a necessary condition for the stationary state but not a sufficient condition. Therefore, the satisfaction of the virial theorem does not necessarily lead to the correct description of the stationary state. For the correct interpretation of Hund's rules, the second- and higher-order corrections in the perturbation expansion are needed, as has been discussed by Colpa and Islip.[17] Both HF and MCHF involve such higher-order corrections as a consequence of self-consistency.

In the present study, we have arrived at the above unified interpretation of the two rules for the $2p$ and $3p$ atoms by both HF and MCHF. The inclusion of correlation does not qualitatively change the HF interpretation of the two rules.[6,7] Correlation necessarily lowers both upper and lower energy levels being compared. The correlation-induced lowering in the energy level is systematically greater for the upper level than for the lower level for both of the two rules.[6,7] An accurate evaluation of correlation in this study leads to a quantitatively good agreement with the experiment.

The reduction of the Hartree screening is caused by two different mechanisms for the two rules. One is due to a greater number of Fermi hole contributions in the higher S states and the other due to the fact that two electrons in the higher L states are more likely to be on opposite sides of the nucleus. V_{en} is lowered at the cost of increasing V_{ee} such that V attains its lowest possible value under the condition of the virial theorem.[6,7]

Finally, we give a brief review of remarkable achievements that some predecessors have made on the correct interpretation of Hund's rules. Davidson is the first who pointed out that electron repulsion is larger for the triplet than for the singlet by performing self-consistent HF calculations of low-lying excited states arising from excited electronic configurations $(1s)^1(ns/np/nd/nf)^1$, $n=2-4$ of the helium atom.[18] Messmer and Birss noticed that the correct interpretation of Hund's first rule is a greater V_{en} so far as the excited states of the helium atom are concerned.[19–21]

A number of quantum chemists have studied Hund's rules for the ground and excited states of the heavier atoms by HF or more elaborate variational methods to demonstrate that the traditional interpretation of Hund's rules is a fallacy.[6,7,15–20,22–32] Their calculations satisfying the virial theorem have arrived at the same conclusion as for the above excited states of the helium atom. So far as neutral species are concerned, Hund's rules are due to a greater V_{en} and V_{ee} is forced to increase in the lower energy state.

As for positively charged isoelectronic systems beyond a certain critical value, it has been understood that although V_{ee} is lower for the lower energy state, the lowering of V_{en} is greater in magnitude than that of V_{ee}, and hence Hund's rules for these positively charged isoelectronic systems are also ascribed to a greater V_{en}. Note that the essential arguments we mentioned above have already been discussed by Katriel and Pauncz in their excellent and detailed 1970s articles and review.[6,7] They explained the role of the contraction of the valence orbitals and expansion of the core orbitals in connection with the crucial role of the virial theorem. Using empirical correlation energies and the Hellmann–Feynman theorem, they also predicted that correlation does not qualitatively change the HF interpretation of Hund's rules but reduces the energy difference between the ground and the excited states. In his variational studies of helium isoelectronic systems, Boyd introduced the concept of *less screening* to explain Hund's spin-multiplicity rule.[30–32]

Since the late 1990s, Koga *et al.* extensively studied Hund's rules for atoms involving a detailed analysis of intracule and extracule densities within the HF framework.[33–36] Nowadays, detailed comparative studies of the interpretation of Hund's multiplicity rule between quantum dots and atoms have been made by Sajeev *et al.*[37] and Sako *et al.*.[38]

Here we introduce a pioneering work by Hartree and Hartree, which was achieved in 1936. They have, for the first time, performed a self-consistent HF calculation for the ^3P and ^1P terms arising from the $1s^2 2s 2p$ excited configuration of the Be atom ($Z=4$).[39] In their study they first found the fact that the exchange term in the HF equation has the effect of reducing the Hartree screening of the nucleus to give rise to the contraction of the valence p orbital, which involves slight expansion of the core s orbitals. Although their HF calculation is accurate enough, regrettably they did not calculate individual energy components of E, V_{en}, V_{ee}, and T. Therefore, one had to wait nearly 30 years to notice that electron repulsion is, in fact, larger for the triplet than for the singlet when in 1964 Davidson first pointed it out. Later, a number of authors have confirmed that both V_{en} and V_{ee} are in magnitude greater for the ^3P term than for the ^1P term of the Be atom.[24,29,34] This fact is due to the above contraction of valence orbitals, and expansion of core orbitals which is called "*LS* term dependence" by Froese Fischer.[40–42]

The earlier studies of Hund's first and second rules for the ground state of heavier neutral atoms have been performed in the framework of the HF theory. It still remains unsettled how correlation affects the HF interpretation of the two rules. In this paper, we give a detailed explanation of how correlation quantitatively changes the HF interpretation of the two rules. The present calculations are accurate enough to satisfy the virial theorem to eight to ten significant figures.

The present paper is organized as follows. In Sec. II we explain the virial theorem. In Sec. III, we give a brief account of numerical HF and MCHF methods and mention a slight modification of the MCHF code we have made in this study. In Sec. IV, we give a unified interpretation of Hund's first and second rules, which is accompanied with a detailed discussion about a role of correlation. Section V is devoted to discussions and Sec. VI to conclusions. Hartree atomic units are used in this paper unless otherwise noted.

II. THE VIRIAL THEOREM

Consider the nonrelativistic Hamiltonian for N-electron atoms,

$$\hat{H} = \hat{T} + \hat{V} = -\frac{1}{2}\sum_{i=1}^{N} \nabla_i^2 - \sum_{i=1}^{N} \frac{Z}{r_i} + \sum_{i>j} \frac{1}{r_{ij}}, \tag{1}$$

where we adopt the adiabatic approximation in which the nucleus mass is regarded as infinity. Z is the nuclear charge and r_i denotes the distance of the ith electron from the nucleus and r_{ij} denotes the distance between the ith and the jth electrons.

The kinetic and the total potential energy operators, $\hat{T}$ and $\hat{V}$ of Hamiltonian (1) are homogeneous in the space coordinates $\boldsymbol{r}$ of degrees −2 and −1, respectively. This means the following scaling properties: $\hat{T}(\{\boldsymbol{r}_i\}) = \lambda^2 \hat{T}(\{\lambda \boldsymbol{r}_i\})$ and $\hat{V}(\{\boldsymbol{r}_i\}) = \lambda \hat{V}(\{\lambda \boldsymbol{r}_i\})$, where λ is a scaling factor. From the spatial scaling properties of $\hat{T}$ and $\hat{V}$, the virial theorem,[5,10,11,43]

$$2T + V = 0, \tag{2}$$

is derived for any stationary state of atoms where T and V are the kinetic and the total potential energies, respectively. The virial theorem is a necessary condition for any stationary state. From the theorem, we are led to

$$E = T + V = -T = V/2 < 0. \tag{3}$$

Compare two stationary states of a many-electron atom. The two states satisfy the virial theorem independently, giving different values of T and V under the condition of the virial ratio, $-V/T = 2$. Hence, the virial relation for the energy differences holds between the two states,

$$2\Delta T + \Delta V = 0 \Leftrightarrow \Delta E = \Delta T + \Delta V = -\Delta T = \Delta V/2. \tag{4}$$

The lower energy state is stabilized by lowering the total potential energy by $\Delta V (= 2\Delta E < 0)$ at the cost of increasing the kinetic energy by $\Delta T (= -\Delta E > 0)$, relative to the higher energy state. The key to understanding how the lower energy state is stabilized lies in analyzing how ΔV becomes negative in terms of its two components, ΔV_{en} and ΔV_{ee}.

The correlation energy E^{corr} is defined by the difference between the exact energy E^{exact} and the HF energy E^{HF},

$$E^{corr} \equiv E^{exact} - E^{HF} < 0. \tag{5}$$

For the proper inclusion of correlation, it is necessary to satisfy the virial relation for the correlation energy. The virial

theorem is satisfied for each of the exact and HF solutions for any stationary state: $2T^{\text{exact}}+V^{\text{exact}}=0$, and $2T^{\text{HF}}+V^{\text{HF}}=0$. Hence, we obtain the correlational virial theorem and the correlational virial relation,

$$2T^{\text{corr}}+V^{\text{corr}}=0 \Leftrightarrow E^{\text{corr}}=-T^{\text{corr}}=V^{\text{corr}}/2<0, \tag{6}$$

where $T^{\text{corr}}\equiv T^{\text{exact}}-T^{\text{HF}}>0$ and $V^{\text{corr}}\equiv V^{\text{exact}}-V^{\text{HF}}<0$. Two components of $V^{\text{corr}}(=V_{\text{en}}^{\text{corr}}+V_{\text{ee}}^{\text{corr}}<0)$ are defined as follows: $V_{\text{en}}^{\text{corr}}\equiv V_{\text{en}}^{\text{exact}}-V_{\text{en}}^{\text{HF}}$ and $V_{\text{ee}}^{\text{corr}}\equiv V_{\text{ee}}^{\text{exact}}-V_{\text{ee}}^{\text{HF}}$.

From Eq. (6), it follows that HF always underestimates the kinetic energy, i.e., $T^{\text{corr}}>0$, by an amount of $|E^{\text{corr}}|$ and overestimates the total potential energy, i.e., $V^{\text{corr}}<0$, by an amount of $2|E^{\text{corr}}|$. In order to satisfy the virial theorem, one must adopt those variational theories that reflect the spatial scaling properties of $\hat{T}$ and $\hat{V}$ of $\hat{H}$. HF and MCHF are suitable for this purpose.

The simultaneous satisfaction of the virial theorem and the Pauli exclusion principle is needed for the correct interpretation of Hund's first and second rules. This is because the effects of the Pauli exclusion principle on the two components V_{en} and V_{ee} in each LS term can be evaluated correctly under the condition of the virial theorem.

Finally, we add that the virial theorem is one of the most important guiding principles for an appropriate evaluation of various electronic properties of stationary states of molecules and solids as well as atoms. The importance of satisfying the virial theorem in the theoretical study of Schrödinger's equation will widely be accepted in the near future just like the Pauli exclusion principle in the *ab initio* calculations for atoms, molecules, and solids.

III. OUTLINE OF NUMERICAL METHODS

In this section, we outline HF and MCHF methods to make some modifications in these codes, which is needed to give a unified interpretation of the first and second rules and to clarify a role of correlation. Detailed reviews of HF and MCHF are given by Froese Fischer.[40–42,44,45]

A. Hartree–Fock method

The HF method[40,46] gives the most accurate independent-particle approximation to the true wavefunction in the variational sense. The HF total wavefunction Ψ has two fundamental properties of the exact total wavefunction ψ, i.e., the virial theorem and the Pauli exclusion principle. As for many-electron atoms, Ψ should be also a simultaneous eigenfunction of the total orbital-, the total spin-angular momentum operators $\hat{\boldsymbol{L}}^2$, $\hat{\boldsymbol{S}}^2$ and their z-components $\hat{L}_z$, $\hat{S}_z$,

$$\hat{\boldsymbol{L}}^2\Psi=L(L+1)\Psi, \quad L=0,1,2,3,\ldots,$$
$$\hat{L}_z\Psi=M_L\Psi, \quad M_L=L,L-1,\ldots,-L+1,-L, \tag{7}$$

$$\hat{\boldsymbol{S}}^2\Psi=S(S+1)\Psi, \quad S=0,\frac{1}{2},1,\frac{3}{2},\ldots,$$
$$\hat{S}_z\Psi=M_S\Psi, \quad M_S=S,S-1,\ldots,-S+1,-S. \tag{8}$$

The orbital- and spin-symmetry adapted HF wavefunction is a linear combination of Slater determinants, and hence is antisymmetric, i.e., satisfying the Pauli principle.[5,10] Such a linear combination is called a configuration-state function (CSF). HF calculations in this study has been performed using the numerical HF program developed by Froese Fischer *et al.*[40,47,48] The radial part of atomic orbitals in the CSF needs to be determined by solving HF equations. In order to satisfy the virial theorem, the HF equations have to be solved independently for both the lower and the higher energy states rather than using the same orbitals obtained for one of them (usually the ground state) to estimate the energy of the other.

B. Multiconfiguration Hartree–Fock method

MCHF[40–42,44,45] is a multiconfiguration approximation to take due account of correlation as a natural extension of HF. The MCHF total wavefunction Ψ is a linear combination of CSFs, $\Phi(\gamma_i LS)$:

$$\psi(\gamma LS)\approx\Psi(\gamma LS)=\sum_{i=1}^{M_{\text{CSF}}}c_i\Phi(\gamma_i LS), \quad \text{where} \sum_{i=1}^{M_{\text{CSF}}}c_i^2=1. \tag{9}$$

M_{CSF} is the number of CSFs and c_i's denote its mixing coefficients. The CSFs in Eq. (9) form an orthonormal set. γ_i in the right-hand side of Eq. (9) is the ith electronic configuration, whereas γ in the left-hand side denotes the dominant electronic configuration within the adopted configurations $\{\gamma_i\}$. A set of $\{\Phi(\gamma_i LS)\}$ consists of the reference configuration (usually the dominant one) and the excited configurations with the same LS symmetry. The excited CSFs are generated by replacing the orbitals in the reference CSF with excited orbitals by 1,2,3,4,… electrons.

The MCHF equations are solved numerically in the same way as HF, except that MCHF requires a self-consistent determination of both mixing coefficients $\{c_i\}$ and radial functions $\{P(nl;r)\}$. If the number of CSFs is only 1, then MCHF is reduced to HF; in this sense MCHF is a natural extension of HF. MCHF is a nonlinear variational method since $\{P(nl;r)\}$ and $\{c_i\}$ are coupled, whereas the configuration interaction (CI) method is a linear variational method since only $\{c_i\}$ are optimized. The MCHF wavefunction satisfying the Pauli exclusion principle is a simultaneous eigenfunction of the operators $\hat{\boldsymbol{L}}^2$, $\hat{\boldsymbol{S}}^2$, $\hat{L}_z$, and $\hat{S}_z$. Furthermore, MCHF satisfies the virial theorem owing to self-consistency.

Note that the atomic orbitals used in the multiconfiguration expansion in Eq. (9) are *not* real atomic orbitals *but* mathematical functions to describe the complicated many-electron wavefunction. Generally, Koopmans' theorem does not hold for these atomic orbitals used in MCHF, excluding exceptional cases such as the two-configuration expansion for the $1s2s$, ^1S excited state of the helium atom where the $2s$ orbital appears only in one CSF.[49]

C. Some computational techniques

In this study, we employed the MCHF ATSP2K code, which has been developed by Froese Fischer *et al.* over many years.[41,45,50–52] Recently, this code has been improved

TABLE I. Number of configuration state functions M_{CSF} used for MCHF (SD,10m) calculations for the $2p$ (C, N, O) and $3p$ (Si, P, S) atoms.

	MCHF (SD,10m)				
C (^3P)	15 240	N (^4S)	7 227	O (^3P)	24 908
C (^1D)	15 946	N (^2D)	36 135	O (^1D)	23 765
C (^1S)	4 496	N (^2P)	24 221	O (^1S)	5 989
Si (^3P)	117 178	P (^4S)	47 630	S (^3P)	138 416
Si (^1D)	109 264	P (^2D)	234 764	S (^1D)	126 990
Si (^1S)	26 958	P (^2P)	153 548	S (^1S)	30 449

by Froese Fischer *et al.* for large-scale MCHF calculations.[53] The improved version enhances the numerical stability in the evaluation of the energy components T and V as compared with the previous version.[41] We have made a slight modification to this improved version for our purpose.

(i) To interpret Hund's first and second rules and make clear the role of correlation based on the virial theorem, we have divided the total potential energy V into its components, V_{en} and V_{ee}.

(ii) To satisfy the virial theorem with desired accuracy, we have checked the convergence of not only E but also T and $V(=V_{en}+V_{ee})$.

(iii) To make clear how exchange and correlation affect the electron density distribution, we have improved the above code so as to evaluate the total radial density distribution $D(r)=4\pi r^2\rho(r)$ and examine its analytic behavior in the immediate vicinity of the nucleus and in the asymptotic region far from the nucleus where $\rho(r)$ is the spherically averaged electron density,

$$\rho(r) \equiv \frac{1}{4\pi}\int \rho(\boldsymbol{r})\mathrm{d}\Omega_r, \tag{10}$$

and $\boldsymbol{r}\equiv(r,\Omega_r)$ represents the position vector with solid angle $\Omega_r\equiv(\theta_r,\phi_r)$. Very recently, Borgoo *et al.* developed a new program that can be added to the above ATSP2K code in order to evaluate not only the electron density $\rho(r)$ but also the natural orbitals.[54] We have checked that the difference of the present $\rho(r)$ with theirs is less than 10^{-11} bohr^{-3} per one electron.[55] The present modification has evaluated $\rho(r)$ directly from the ATSP2K code to avoid numerical errors.

In all the present MCHF calculations, the maximum orbital-angular momentum used in the active space is $l=n-1$, where n is the maximum principal quantum number. In order to give a unified interpretation of Hund's first and second rules, we have performed MCHF calculations including single and double excitations using 55 atomic orbitals {1s, 2s, 2p, …, 10i, 10k, 10l, 10m} in the active space. Here, we abbreviate this scale of calculation to MCHF(SD,10m). For comparison, we have also performed MCHF(SDT,8k) and MCHF(SDTQ,5g) calculations for the carbon atom, where SDT and SDTQ stand for single-double-triple and single-double-triple-quadruple excitations, respectively. MCHF(SD,10m) favorably compares with other accurate methods, which will be discussed in Sec. IV A.

Table I gives a list of the number of CSFs M_{CSF} in MCHF (SD,10m) for the $2p$ (C, N, O) and $3p$ (Si, P, S) atoms. Table II shows the number of CSFs for the carbon atom in MCHF(SD,nl), MCHF(SDT,nl), and MCHF(SDTQ,nl) for two sets of the active space, i.e., {1s, 2s,…, 5g} with 15 orbitals and {1s, 2s, …, 8k} with 36 orbitals. In our study of the carbon atom, MCHF(SDT,8k) and MCHF(SDTQ,5g) are the available largest scale calculations for SDT and SDTQ excitations, respectively.

All the MCHF(SD,10m) calculations for the $2p$ atoms were performed using a serial version of the ATSP2K code (1 CPU). On the other hand, for the $3p$ atoms, a parallel (MPI) version of the ATSP2K code was employed with 16 CPUs parallelization to distribute the memory load, especially for the ^3P and ^1D terms of Si and S, as well as the ^2D and ^2P terms of P. The most difficult problem with large-scale MCHF calculations is *not* computational time *but* memory load. We have overcome this problem with the help of parallel-computer. Both MCHF(SDT,8k) and MCHF(SDTQ,5g) calculations for the carbon atom were carried out with 64 CPUs parallelization. The present large-scale MCHF calculations have been performed on a HITACHI SR11000 supercomputer.

IV. NUMERICAL RESULTS

To begin with, we discuss how the MCHF calculation we have performed in this study is accurate in its treatment of the correlation energy.

TABLE II. Number of configuration state functions M_{CSF} used for MCHF calculations including SD, SDT, and SDTQ excitations for the carbon atom. M_{CSF} used for two cases of active set, {1s, 2s,…,5g} and {1s, 2s,…,8k} is given.

MCHF	(SD,5g)	(SDT,5g)	(SDTQ,5g)
C (^3P)	1290	21 664	171 975
C (^1D)	1186	18 587	145 208
C (^1S)	431	5 345	38 212
MCHF	(SD,8k)	(SDT,8k)	(SDTQ,8k)
C (^3P)	7195	424 441	(12 138 522)[a]
C (^1D)	7302	394 879	(10 934 752)[a]
C (^1S)	2186	95 630	(2 477 588)[a]

[a]MCHF(SDTQ,8k) is not performed in this study.

TABLE III. The total energy E obtained from HF, MCHF(SD,10m) and the estimated exact for (a) $2p$ (C, N, O) and (b) $3p$ (Si, P, S) atoms. The calculated correlation energy E^{corr} together with its recovering percentage $\%E^{corr}$ relative to the estimated exact correlation energy is also given for MCHF(SD,10m). All energies are in hartree units.

Atom (Term)	HF	MCHF (SD,10m)			Estimated exact[a,b]		
	E	E	E^{corr}	$\%E^{corr}$	E	E^{corr}	$\%E^{corr}$
			(a) $2p$ atoms				
C (^3P)	−37.688 62	−37.839 72	−0.1511	96.6	−37.845 00	−0.1564	100
C (^1D)	−37.631 33	−37.792 77	−0.1614	96.5	−37.798 56	−0.1672	100
C (^1S)	−37.549 61	−37.738 64	−0.1890	96.1	−37.746 36	−0.1968	100
N (^4S)	−54.400 93	−54.582 53	−0.1816	96.5	−54.589 20	−0.1883	100
N (^2D)	−54.296 17	−54.493 63	−0.1975	96.1	−54.501 61	−0.2054	100
N (^2P)	−54.228 10	−54.448 16	−0.2201	95.8	−54.457 80	−0.2297	100
O (^3P)	−74.809 40	−75.055 88	−0.2465	95.6	−75.067 30	−0.2579	100
O (^1D)	−74.729 26	−74.983 60	−0.2543	95.7	−74.995 00	−0.2657	100
O (^1S)	−74.611 02	−74.900 64	−0.2896	95.8	−74.913 33	−0.3023	100
			(b) $3p$ atoms				
Si (^3P)	−288.854 36	−289.322 58	−0.4682	92.8	−289.359 00	−0.5046	100
Si (^1D)	−288.815 21	−289.290 98	−0.4758	92.4	−289.330 30	−0.5151	100
Si (^1S)	−288.759 09	−289.244 10	−0.4850	91.4	−289.288 86	−0.5298	100
P (^4S)	−340.718 78	−341.219 67	−0.5009	92.7	−341.259 00	−0.5402	100
P (^2D)	−340.648 87	−341.162 72	−0.5139	92.0	−341.207 24	−0.5584	100
P (^2P)	−340.603 30	−341.124 61	−0.5213	91.4	−341.173 69	−0.5704	100
S (^3P)	−397.504 90	−398.060 80	−0.5559	91.9	−398.110 00	−0.6051	100
S (^1D)	−397.452 35	−398.016 73	−0.5644	91.7	−398.067 91	−0.6156	100
S (^1S)	−397.374 68	−397.951 63	−0.5769	91.0	−398.008 94	−0.6343	100

[a]Chakravorty *et al.* (Ref. 57).
[b]NIST Atomic Spectra Database (Ref. 58).

A. The recovering percentage of the correlation energy

Table III shows a list of numerical values for the $2p$ (C, N, O) and $3p$ (Si, P, S) atoms, i.e., the total energy E, the correlation energy E^{corr}, and the recovering percentage of the correlation energy $\%E^{corr}$ evaluated from HF and MCHF(SD,10m). "Estimated exact energy" E^{exact} for the ground terms in the table means "exact nonrelativistic energy" estimated by Davidson and Chakravorty *et al.*,[56,57] which is the most reliable nonrelativistic energy for the ground state of second and third row atoms in the Periodic Table. E^{exact} for the excited terms is estimated by a combination of the above E^{exact} for the ground term and the experimental energy differences ΔE^{expt} between the ground and excited LS terms.[58]

Here, we assume that relativistic effects do not change the energy differences ΔE between various LS terms arising from the same electronic configuration. The validity of this assumption can be confirmed from a comparison of the relativistic correction E^{rel} of the LS terms in the HF framework; e.g., E^{rel} for the carbon atom is $E^{rel}(^3P) = -0.013\,672$ hartree, $E^{rel}(^1D) = -0.013\,675$ hartree, and $E^{rel}(^1S) = -0.013\,681$ hartree. The differences of E^{rel} between the LS terms arising from the same configuration are of the order of $10^{-7}-10^{-6}$ hartree for the $2p$ atoms and $10^{-6}-10^{-5}$ hartree for the $3p$ atoms.

"Exact correlation energy" in Table III is evaluated by subtracting the numerical HF energy E^{HF} from the exact energy E^{exact}. We show the recovering percentage of the correlation energy $\%E^{corr}$ relative to the exact correltaion energy (100%) to demonstrate the accuracy of the present MCHF calculations. MCHF(SD,10m) attains about 96% of the exact correlation energy for the $2p$ atoms, much higher than 90.0%–93.4% evaluated in our previous diffusion Monte Carlo (DMC) studies;[1,2] these studies adopt the fixed-node approximation in which the nodal part is constructed from a single Slater determinant. $\%E^{corr}$ of MCHF(SD,10m) for the $3p$ atoms are about 92%, which is of almost the same accuracy as in our previous DMC studies.

It has been recognized that the lower values of $\%E^{corr}$ for the Be–O atoms in the fixed-node DMC with a single Slater determinant is ascribed to the fact that it fails to take full account of the so-called "$2s-2p$ near degeneracy effect." Recently, Buendía *et al.* explained the $ns-np$ near degeneracy effect on the DMC energy for the Li–Ar atoms by comparing single- and multi-determinant DMC within the fixed-node approximation.[59] So far as single-determinant DMC within the fixed-node approximation is concerned, a similar trend in the variation of $\%E^{corr}$ for the Li–Ar atoms is also observed in our preliminary calculations.

Table IV shows the same list as Table III for the ^3P, ^1D, and ^1S terms of the carbon atom evaluated from two different scale MCHF calculations, i.e., MCHF(SDT,8k) and MCHF(SDTQ,5g). MCHF(SDT,8k) attains about 97%–98% of the exact correlation energy for the carbon atom. MCHF(SDT,8k) and the estimated exact values show an excellent agreement to within four significant figures. The present MCHF(SDTQ,nl) does not involve those orbitals that

TABLE IV. E, E^{corr}, and $\%E^{corr}$ obtained from MCHF(SDT,8k), MCHF(SDTQ,5g), and SDTQ-CI for the carbon atoms. All energies are in hartree units.

Atom (Term)	MCHF(SDT,8k)			MCHF(SDTQ,5g)			SDTQ-CI[a]		
	E	E^{corr}	$\%E^{corr}$	E	E^{corr}	$\%E^{corr}$	E	E^{corr}	$\%E^{corr}$
C (^3P)	−37.841 83	−0.1532	98.0	−37.834 32	−0.1457	93.2	−37.839 30	−0.1507	96.4
C (^1D)	−37.795 23	−0.1639	98.0	−37.786 77	−0.1554	92.9	−37.792 40	−0.1611	96.3
C (^1S)	−37.741 04	−0.1914	97.3	−37.733 89	−0.1843	93.7	−37.738 50	−0.1889	96.0

[a]Sasaki and Yoshimine (Ref. 60).

are higher than 5g because of a huge number of CSFs. MCHF(SDTQ,5g) attains about 93% of the exact correlation energy for the carbon atom. Larger scale parallel-computing environments in the near future will enable one to perform much larger scale MCHF calculations, involving the higher orbitals for SDT, SDTQ,…excitations to attain more than 99% of the exact correlation energy.

For comparison, we also show in Table IV the SDTQ-CI result for the ^3P, ^1D, and ^1S terms arising from the $1s^22s^22p^2$ configuration of the carbon atom. These calculations have been performed by Sasaki and Yoshimine[60] in 1974 using the ALCHEMY code with 35 atomic orbitals expanded in terms of optimized Slater-type functions $[10s9p8d8f6g4h2i]$. They included all the SD excited configurations but selected only those triple-quadruple excited configurations that make an important contribution to E^{corr}. The numbers of CSFs in their CI expansion are 993 (735 SD+257 TQ) for ^3P, 953 (740 SD+212 TQ) for ^1D, and 756 (644 SD+111 TQ) for ^1S. Within the computational capability of 1970s, they obtained a surprisingly high recovering percentage of the correlation energy, which are accepted as a highly accurate record even today. However, the accuracy of the virial ratio $-V/T$ as well as the energy components V_{en}, V_{ee}, and T is not reported in their calculations.

The present study of MCHF(SD,10m) not only gives the higher $\%E^{corr}$ than their SDTQ-CI but also leads to a remarkably high accuracy in the virial ratio $-V/T=2$ for the $2p$ (C, N, O) and the $3p$ (Si, P, S) atoms. The energy difference virial ratio $-\Delta V/\Delta T=2$ and the correlational virial ratio $-V^{corr}/T^{corr}=2$ are both evaluated with high accuracy.

In Sec. IV B, we explain why the accurate satisfaction of $-\Delta V/\Delta T=2$ and $-V^{corr}/T^{corr}=2$ is essential for a unified interpretation of Hund's first and second rules and the correct description of the role of correlation.

B. Individual energy components

For a unified interpretation of Hund's first and second rules, it is necessary to make a detailed analysis of the total energy into the individual energy components V_{ee}, V_{en}, and T under the condition $2T+V=0$. Table V gives a list of numerical values of the total energy E and its components V_{ee}, V_{en}, and T for the $2p$ (C, N, O) atoms calculated by HF and MCHF(SD,10m). Table VI gives the same list for the $3p$ (Si, P, S) atoms. The virial ratio $-V/T$ is also given in the last column of each table. The present HF calculations satisfy the virial ratio $-V/T=2$ to eight to nine significant figures. It is difficult for the Hartree–Fock–Roothaan method with a moderate basis set to attain such accuracy.

As has been mentioned in Sec. III C, we have made a slight modification of the MCHF code. By this modification, we have succeeded to optimize the MCHF wavefunction,

TABLE V. HF and MCHF(SD,10m) energies and the virial ratio $-V/T$ for the $2p$ (C, N, O) atoms. All energies are in hartree units.

Atom	Method	State	E	V_{ee}	V_{en}	T	Virial ratio
C ($Z=6$)	HF	^3P	−37.688 618 95	12.759 645 96	−88.136 883 76	37.688 618 84	2.000 000 002 9
$[He]2s^22p^2$		^1D	−37.631 331 26	12.728 306 12	−87.990 968 69	37.631 331 31	1.999 999 998 7
		^1S	−37.549 610 85	12.666 966 57	−87.766 188 15	37.549 610 72	2.000 000 003 6
	MCHF	^3P	−37.839 723 85	12.533 700 50	−88.213 148 18	37.839 723 84	2.000 000 000 3
	(SD,10m)	^1D	−37.792 769 14	12.485 083 62	−88.070 621 91	37.792 769 15	1.999 999 999 8
		^1S	−37.738 638 13	12.423 142 63	−87.900 418 80	37.738 638 04	2.000 000 002 3
N ($Z=7$)	HF	^4S	−54.400 934 19	19.549 399 14	−128.351 267 37	54.400 934 04	2.000 000 002 8
$[He]2s^22p^3$		^2D	−54.296 169 33	19.510 080 95	−128.102 419 45	54.296 169 17	2.000 000 002 9
		^2P	−54.228 101 84	19.478 339 94	−127.934 543 60	54.228 101 81	2.000 000 000 6
	MCHF	^4S	−54.582 527 71	19.247 536 10	−128.412 591 52	54.582 527 71	2.000 000 000 0
	(SD,10m)	^2D	−54.493 633 08	19.178 576 61	−128.165 842 72	54.493 633 03	2.000 000 000 9
		^2P	−54.448 161 29	19.137 459 46	−128.033 781 93	54.448 161 18	2.000 000 002 0
O ($Z=8$)	HF	^3P	−74.809 398 45	28.455 830 66	−178.074 627 37	74.809 398 26	2.000 000 002 4
$[He]2s^22p^4$		^1D	−74.729 264 26	28.427 224 05	−177.885 752 55	74.729 264 23	2.000 000 000 4
		^1S	−74.611 020 63	28.378 355 57	−177.600 396 65	74.611 020 45	2.000 000 002 5
	MCHF	^3P	−75.055 882 97	28.018 638 20	−178.130 404 01	75.055 882 85	2.000 000 001 7
	(SD,10m)	^1D	−74.983 603 84	27.980 298 50	−177.947 506 11	74.983 603 76	2.000 000 001 0
		^1S	−74.900 643 33	27.917 867 75	−177.719 154 25	74.900 643 18	2.000 000 002 0

TABLE VI. HF and MCHF(SD,10m) energies and the virial ratio $-V/T$ for the $3p$ (Si, P, S) atoms. All energies are in hartree units.

Atom	Method	State	E	V_{ee}	V_{en}	T	Virial ratio
Si (Z=14)	HF	^3P	−288.854 362 42	111.706 136 90	−689.414 861 51	288.854 362 19	2.000 000 000 8
[Ne]$3s^2 3p^2$		^1D	−288.815 207 70	111.592 628 10	−689.223 043 14	288.815 207 34	2.000 000 001 2
		^1S	−288.759 085 02	111.402 670 43	−688.920 840 20	288.759 084 75	2.000 000 000 9
	MCHF	^3P	−289.322 578 85	111.070 906 03	−689.716 063 11	289.322 578 23	2.000 000 002 2
	(SD,10m)	^1D	−289.290 977 33	110.977 246 53	−689.559 200 69	289.290 976 83	2.000 000 001 7
		^1S	−289.244 099 95	110.818 448 11	−689.306 647 44	289.244 099 39	2.000 000 001 9
P (Z=15)	HF	^4S	−340.718 780 85	130.783 451 84	−812.221 013 28	340.718 780 59	2.000 000 000 8
[Ne]$3s^2 3p^3$		^2D	−340.648 870 43	130.638 070 63	−811.935 811 07	340.648 870 01	2.000 000 001 3
		^2P	−340.603 303 82	130.534 682 23	−811.741 289 59	340.603 303 55	2.000 000 000 8
	MCHF	^4S	−341.219 668 81	130.101 680 97	−812.541 018 09	341.219 668 30	2.000 000 001 5
	(SD,10m)	^2D	−341.162 720 70	129.973 059 88	−812.298 500 76	341.162 720 18	2.000 000 001 5
		^2P	−341.124 605 28	129.882 694 89	−812.131 905 40	341.124 605 23	2.000 000 000 2
S (Z=16)	HF	^3P	−397.504 895 77	151.883 834 25	−946.893 625 44	397.504 895 42	2.000 000 000 9
[Ne]$3s^2 3p^4$		^1D	−397.452 353 66	151.791 997 64	−946.696 705 42	397.452 354 11	1.999 999 998 9
		^1S	−397.374 680 03	151.647 788 43	−946.397 149 88	397.374 681 42	1.999 999 996 5
	MCHF	^3P	−398.060 798 92	151.156 285 99	−947.277 883 57	398.060 798 66	2.000 000 000 7
	(SD,10m)	^1D	−398.016 731 28	151.074 035 71	−947.107 499 21	398.016 732 22	1.999 999 997 6
		^1S	−397.951 625 73	150.949 902 80	−946.853 156 17	397.951 627 64	1.999 999 995 2

paying special attention to the convergence of T and $V(=V_{en}+V_{ee})$ as well as E to attain a sufficient accuracy in the virial ratio $-V/T=2$. As a result, we have succeeded to satisfy $-V/T=2$ systematically to eight to ten significant figures.[61]

From our practical experience, it seems that MCHF tends to give a more accurate virial ratio than HF. This is probably because the MCHF wavefunction has much more flexibility coming from a set of $P(nl;r)$ and a large set of c_i, whereas the HF wavefunction has less flexibility from a set of $P(nl;r)$ alone. The same HF code has also been modified by Koga *et al.*[35] Their values of E^{HF} are about $10^{-7}-10^{-9}$ hartree lower (better) than the present HF values for all the atoms calculated. Their virial ratio is also better than the present one. For some atoms, the accuracy of their virial ratio $(-V/T=2)$ exceeds 15 significant figures.

It should be emphasized that even if an improvement in the total energy $|\delta E|$ is negligibly small between nth and $n+1$th SCF iterations, the corresponding improvement in the two energy components, T and V, is significantly large in order to approach the virial ratio $-V/T=2$ by iteration. This is because the convergence of T and V in each iteration is slower than that of $E(=T+V)$. To satisfy the virial theorem accurately, it is necessary to continue the SCF procedure even if E seems to converge. The importance of the self-consistency above has also been pointed out by Froese Fischer.[41,62]

The correct interpretation of Hund's rules, in fact, requires sufficiently accurate convergence of T and V. Both the traditional and the correct interpretations give almost the same E, but its components V_{ee}, V_{en}, and T are essentially different between the two (see also a discussion given by Katriel and Pauncz.[6,7])

With the above situation in mind, we conclude that the satisfaction of the virial theorem $2T+V=0$ is the proper criterion to judge real convergence of self-consistent calculations far beyond seeming convergence of the total energy E. The satisfaction of the virial theorem should be accepted as the proper criterion for *ab initio* self-consistent calculations.

From both MCHF and HF, we have arrived at the following inequalities for the ns^2np^2 configuration of the C and Si atoms,

$$\begin{aligned} &E(^3P) < E(^1D) < E(^1S) < 0, \\ &V_{en}(^3P) < V_{en}(^1D) < V_{en}(^1S) < 0, \\ &T(^3P) > T(^1D) > T(^1S) > 0, \\ &V_{ee}(^3P) > V_{ee}(^1D) > V_{ee}(^1S) > 0. \end{aligned} \tag{11}$$

The same inequalities hold for the ns^2np^4 configuration of the O and S atoms. Similar four inequalities hold for the ns^2np^3 configuration of the N and P atoms,

$$\begin{aligned} &E(^4S) < E(^2D) < E(^2P) < 0, \\ &V_{en}(^4S) < V_{en}(^2D) < V_{en}(^2P) < 0, \\ &T(^4S) > T(^2D) > T(^2P) > 0, \\ &V_{ee}(^4S) > V_{ee}(^2D) > V_{ee}(^2P) > 0. \end{aligned} \tag{12}$$

Note that all the inequalities (11) and (12) hold regardless of whether calculations are performed with or without correlation. A unified interpretation of Hund's first and second rules for the $2p$ and $3p$ atoms is derived from the sets of the inequalities (11) and (12). Both the first and second rules are ascribed to a greater V_{en} that is gained at the cost of increasing V_{ee}.

In general, the more stable LS term has the lower (more negative) value of V_{en} and the higher (more positive) value of V_{ee}, compared to the other LS terms arising from the same

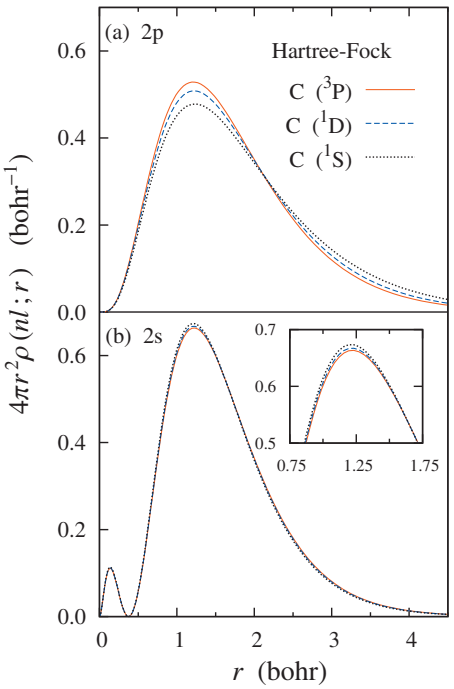

FIG. 1. Comparison of the radial density distribution $4\pi r^2\rho(nl;r)$ from (a) the $2p$ orbital and (b) the $2s$ orbital calculated by HF for the ^3P, ^1D, and ^1S terms of the carbon atom.

configuration. In principle, two other ways of stabilizing V are possible: (a) $\Delta V_{\rm en}<0$, $\Delta V_{\rm ee}<0$ and (b) $\Delta V_{\rm en}>0$, $\Delta V_{\rm ee}<0$. So far as the ground configurations of the neutral atoms are concerned, cases (a) and (b) are not observed. As for excited configurations of the neutral atoms, a very small number of the above cases (a) and (b) have been reported within the framework of HF by Koga *et al.*[36] Note that the purpose of their extensive study is to demonstrate the general conclusion that the ground *LS* term has the largest values of $|V_{\rm en}|$ and $|V_{\rm ee}|$ as compared with the other *LS* terms arising from the same configuration.

To obtain a better understanding, we shall analyze how the above inequalities (11) and (12) are related to various contributions from different orbitals to $V_{\rm en}$ and $V_{\rm ee}$.[61] HF enables one to perform such an orbital analysis because it defines physically meaningful one-electron orbitals. On the other hand, at present, it is difficult to define physically meaningful orbitals in MCHF.

Figure 1 compares the radial density distribution $4\pi r^2\rho(2s;r)$ and $4\pi r^2\rho(2p;r)$ from the $2s$ and $2p$ orbitals for the ^3P, ^1D, and ^1S terms of the carbon atom, calculated with HF. For convenience, the spherically averaged one-electron density distribution of nl-shell, $\rho(nl;r)$ is renormalized to unity for each subshell, regardless of the number of electrons involved. Obviously, $4\pi r^2\rho(2p;r)$ more contracts toward the nucleus for the more stable *LS* term. In other words, the magnitude of $4\pi r^2\rho(2p;r)$ becomes larger in the order ^3P, ^1D, and ^1S for $0<r<2.1$ bohrs and smaller in the same order for $r>2.1$. The penetration of the $2p$ orbitals into the immediate vicinity of the nucleus causes an *extra screening* of the nucleus to give a slight but significant expansion of the $1s$ and $2s$ core orbitals.[6,7] Hence, the magnitude of $4\pi r^2\rho(2s;r)$ becomes smaller in the order ^3P, ^1D, and ^1S for $0<r<1.6$ bohrs and larger in the same order for $r>1.6$.

In Fig. 1, the $1s$ orbital is not shown because the expansion of the $1s$ electron density distribution is vanishingly small (less than 10^{-5} bohrs^{-1}). We have observed both contraction of the $2p$ orbitals and expansion of the $2s$ and $1s$ core orbitals in the more stable *LS* terms of all the $2p$ (C, N, O) atoms. A similar combination of contraction of the $3p$ and $2p$ orbitals and expansion of the $3s$, $2s$, and $1s$ core orbitals has been observed for the more stable *LS* terms of all the $3p$ (Si, P, S) atoms.

From a systematic HF analysis of $\Delta V_{\rm en}=\Sigma_{nl}\Delta V_{\rm en}^{(nl)}$ into its orbital contributions $\Delta V_{\rm en}^{(nl)}$ for the $2p$ and $3p$ atoms, we have confirmed that the largest contribution to lower $V_{\rm en}$ in the more stable *LS* term is a contraction of the outermost valence p orbitals, i.e., $2p$ orbital for the $2p$ atoms and $3p$ orbital for the $3p$ atoms. As for the $3p$ atoms, it should be noted that *not all* the core orbitals expand in the more stable state. So far as the $2p$ and $3p$ atoms are concerned, the p orbitals ($l=1$) give rise to a contraction whereas the s orbitals ($l=0$) give a slight but significant expansion in the more stable state.[6,7]

The same interpretation of Hund's rule has been confirmed for the methylene molecule, CH_2.[63] The stabilization of the $^3B_1$ state relative to the $^1B_1$ state of CH_2 is ascribed to a similar contraction of the valence orbitals ($3a_1$ and $1b_1$), which involves an expansion of the core orbitals ($1a_1$, $2a_1$, and $1b_2$).

Hund's first rule is ascribed to the fact that individual exchange terms in the highest spin-multiplicity state are most efficient in reducing the Hartree screening of the nucleus. Let us term this effect "exchange-induced reduction in screening." On the other hand, the second rule is ascribed to another type of the *reduced screening* because the two *LS* terms being compared have the same value of spin-multiplicity (see Sec. IV C).

By an analogous way of decomposing $\Delta V_{\rm en}$, we have decomposed $\Delta V_{\rm ee}$ into its orbital-pair contributions $\Delta V_{\rm ee}^{(nl-n'l')}$. Interestingly, we have found that the mechanism of how the total $V_{\rm ee}$ becomes larger in the more stable *LS* terms is common to both Hund's first and second rules for the $2p$ and $3p$ atoms.

For the $2p$ atoms, there are six different types of the electron-electron interaction components $V_{\rm ee}^{(nl-n'l')}$. The increase in the electron-electron interaction is larger for the $1s-2p$ than for the $2s-2p$ interaction ($\Delta V_{\rm ee}^{(1s-2p)}>\Delta V_{\rm ee}^{(2s-2p)}>0$). This trend is common to the first and second rules for all the $2p$ atoms. The reason for the above inequality is that the $1s$ orbital has no node in the radial part, whereas the $2s$ orbital has one node. The decrease in the $2p-2p$ interaction is the greatest. The decreasing order of the electron-electron interaction is as follows: $\Delta V_{\rm ee}^{(2p-2p)}<\Delta V_{\rm ee}^{(1s-2s)}<\Delta V_{\rm ee}^{(2s-2s)}<\Delta V_{\rm ee}^{(1s-1s)}<0$.

For the $3p$ atoms, there are 15 different types of the components $V_{\rm ee}^{(nl-n'l')}$. For convenience, we term an orbital whose energy is lower than those of other orbitals in a neutral $3p$ atom as "the more inner orbital." Namely, the order of the more inner orbital is as follows: $1s,2s,2p,3s,3p$.

In the more stable *LS* term, the interaction between the

TABLE VII. Correlation energy components calculated as the difference between MCHF(SD,10m) and HF and the correlational virial ratio $-V^{\mathrm{corr}}/T^{\mathrm{corr}}$ for the $2p$ atoms (C, N, O) and the $3p$ atoms (Si, P, S). All energies are in hartree units.

Atom	State	E^{corr}	$V_{\mathrm{ee}}^{\mathrm{corr}}$	$V_{\mathrm{en}}^{\mathrm{corr}}$	T^{corr}	$-V^{\mathrm{corr}}/T^{\mathrm{corr}}$
			(a) $2p$ atoms			
C ($Z=6$)	^3P	−0.151 104 9	−0.225 945 5	−0.076 264 4	0.151 105 0	1.999 999 4
$[\mathrm{He}]2s^2 2p^2$	^1D	−0.161 437 9	−0.243 222 5	−0.079 653 2	0.161 437 8	2.000 000 3
	^1S	−0.189 027 3	−0.243 823 9	−0.134 230 7	0.189 027 3	1.999 999 7
N ($Z=7$)	^4S	−0.181 593 5	−0.301 863 0	−0.061 324 2	0.181 593 7	1.999 999 2
$[\mathrm{He}]2s^2 2p^3$	^2D	−0.197 463 8	−0.331 504 3	−0.063 423 3	0.197 463 9	1.999 999 5
	^2P	−0.220 059 4	−0.340 880 5	−0.099 238 3	0.220 059 4	2.000 000 4
O ($Z=8$)	^3P	−0.246 484 5	−0.437 192 5	−0.055 776 6	0.246 484 6	1.999 999 8
$[\mathrm{He}]2s^2 2p^4$	^1D	−0.254 339 6	−0.446 925 5	−0.061 753 6	0.254 339 5	2.000 000 2
	^1S	−0.289 622 7	−0.460 487 8	−0.118 757 6	0.289 622 7	1.999 999 9
			(b) $3p$ atoms			
Si ($Z=14$)	^3P	−0.468 216 4	−0.635 230 9	−0.301 201 6	0.468 216 0	2.000 000 8
$[\mathrm{Ne}]3s^2 3p^2$	^1D	−0.475 769 6	−0.615 381 6	−0.336 157 5	0.475 769 5	2.000 000 3
	^1S	−0.485 014 9	−0.584 222 3	−0.385 807 2	0.485 014 6	2.000 000 6
P ($Z=15$)	^4S	−0.500 888 0	−0.681 770 9	−0.320 004 8	0.500 887 7	2.000 000 5
$[\mathrm{Ne}]3s^2 3p^3$	^2D	−0.513 850 3	−0.665 010 8	−0.362 689 7	0.513 850 2	2.000 000 2
	^2P	−0.521 301 5	−0.651 987 3	−0.390 615 8	0.521 301 7	1.999 999 6
S ($Z=16$)	^3P	−0.555 903 1	−0.727 548 3	−0.384 258 1	0.555 903 2	1.999 999 8
$[\mathrm{Ne}]3s^2 3p^4$	^1D	−0.564 377 6	−0.717 961 9	−0.410 793 8	0.564 378 1	1.999 999 1
	^1S	−0.576 945 7	−0.697 885 6	−0.456 006 3	0.576 946 2	1.999 999 1

contracted/expanded orbital and the more inner orbital contributes to an increase/decrease in ΔV_{ee}. If two equivalent orbitals in question contract/expand in the more stable LS term, the interaction between equivalent orbitals, $V_{\mathrm{ee}}^{(nl-nl)}$ contributes to an increase/decrease in ΔV_{ee}. However, the interaction between the two valence p orbitals makes a contribution to a decrease in ΔV_{ee} in spite of the contraction. For the first rule, this is because of a larger number of Fermi hole contributions and for the second rule, a larger probability that two electrons are more likely to be on opposite sides of the nucleus.

The above rule found for the $3p$ atoms concerning whether $\Delta V_{\mathrm{ee}}^{(nl-n'l')}$ increases or decreases also applies to the $2p$ atoms. An exception of this rule is the $2s-2p$ interaction in the silicon atom. This interaction contributes to a decrease in ΔV_{ee} in the more stable LS term, although the magnitude of $\Delta V_{\mathrm{ee}}^{(2s-2p)}$ is vanishingly small, i.e., less than 10^{-4} hartree.

Lemberger and Pauncz already reported a similar analysis of V_{ee} into the shell contributions for the ^3P, ^1D, and ^1S terms of the carbon atom.[22] They used a Roothaan SCF wavefunction due to Clementi to decompose V_{ee} into the closed-shell, intershell, and open-shell contributions. The present numerical HF analysis of V_{ee} is consistent with their HF-Roothaan analysis.

C. Correlation effects on the energy components

In this section we discuss the correlation effect on the energy components V_{ee}, V_{en}, and T. Table VII gives a list of E^{corr} and its components $V_{\mathrm{ee}}^{\mathrm{corr}}$, $V_{\mathrm{en}}^{\mathrm{corr}}$, and T^{corr} for each of the LS terms of the $2p$ and $3p$ atoms, which are evaluated as the difference between the MCHF(SD,10m) and the HF calculations. In the present study, the correlational virial ratio is accurate to six significant figures, i.e., $-V^{\mathrm{corr}}/T^{\mathrm{corr}}=2.000\,000$ for all the $2p$ and $3p$ atoms. As shown in Table III, the recovery percentage of the correlation energy $\%E^{\mathrm{corr}}$ is sufficiently high: $\%E^{\mathrm{corr}}$ is about 95%–96% for the $2p$ atoms and 91%–92% for the $3p$ atoms. Hence, we may conclude that each of the correlation components is qualitatively correct and quantitatively reliable.

We have arrived at the following inequalities for every LS term of all the $2p$ and $3p$ atoms:

$$\begin{aligned} E^{\mathrm{MCHF}} &< E^{\mathrm{HF}}, \\ V_{\mathrm{ee}}^{\mathrm{MCHF}} &< V_{\mathrm{ee}}^{\mathrm{HF}}, \\ V_{\mathrm{en}}^{\mathrm{MCHF}} &< V_{\mathrm{en}}^{\mathrm{HF}}, \\ T^{\mathrm{MCHF}} &> T^{\mathrm{HF}}. \end{aligned} \tag{13}$$

Correlation lowers V_{ee} ($V_{\mathrm{ee}}^{\mathrm{corr}}<0$) by forming the so-called Coulomb hole and deepening the Fermi hole. Correlation also lowers V_{en} ($V_{\mathrm{en}}^{\mathrm{corr}}<0$) by reducing the Hartree–Fock nuclear screening at short interelectronic distances to contract the electron density distribution toward the nucleus as a whole. This property may be termed as *correlation-induced reduction in screening*, which is to be compared with *exchange-induced reduction in screening*. Correlation inevitably increases T ($T^{\mathrm{corr}}>0$) by increasing the curvature of the many-electron wavefunction in two ways. One is due to the correlational motion between electrons and the other is due to correlation-induced contraction of the electron density distribution toward the nucleus. The three correlation effects above are connected through the correlational virial theorem $2T^{\mathrm{corr}}+V_{\mathrm{en}}^{\mathrm{corr}}+V_{\mathrm{ee}}^{\mathrm{corr}}=0$.

In 1969, Lemberger and Pauncz investigated Hund's first and second rules for the carbon atom by HF-Roothaan and doubly excited CI methods[22] to arrive at the same inequalities as Eq. (11). However, they could not correctly evaluate the above correlation-induced increase in T and lowering in V_{en} since their calculation did not satisfy the correlational virial theorem. The main reason for their failure is that the correlation contribution from single excitations was not involved. This is probably because computational power of those days was insufficient. Although the inclusion of single excitations in CI makes a minor contribution to E^{corr} itself, it makes a significant contribution to one-electron properties such as the electron density distribution as well as V_{en} and T through a possible change in the mixing coefficients caused by the inclusion of single excitations. Their inappropriate results of $T^{corr}<0$ and $V_{en}^{corr}>0$ come from an insufficient description of the correlation-induced contraction of the electron density distribution.

Let us make a quantitative comparison of correlation effects between LS terms listed in Table VII. We have arrived at the following inequalities for $E^{corr}(=-T^{corr})$, common to the $2p$ and $3p$ atoms studied:

$$E^{corr}(^1S) < E^{corr}(^1D) < E^{corr}(^3P) < 0,$$
$$T^{corr}(^1S) > T^{corr}(^1D) > T^{corr}(^3P) > 0. \tag{14}$$

On the other hand, we have arrived at the following inequalities for the two components of $V^{corr}(=V_{en}^{corr}+V_{ee}^{corr}=2E^{corr})$ in the $2p$ atoms:

$$V_{ee}^{corr}(^1S) < V_{ee}^{corr}(^1D) < V_{ee}^{corr}(^3P) < 0,$$
$$V_{en}^{corr}(^1S) < V_{en}^{corr}(^1D) < V_{en}^{corr}(^3P) < 0, \tag{15}$$

and in the $3p$ atoms,

$$V_{ee}^{corr}(^3P) < V_{ee}^{corr}(^1D) < V_{ee}^{corr}(^1S) < 0,$$
$$V_{en}^{corr}(^1S) < V_{en}^{corr}(^1D) < V_{en}^{corr}(^3P) < 0. \tag{16}$$

Similar inequalities hold for the N and P atoms if one replaces ^3P, ^1D, and ^1S in inequalities (14)–(16) by ^4S, ^2D, and ^2P.

Inequality (14) can be interpreted in a straightforward manner: the reason why $|E^{corr}|$ is greater in ^1D $(S=0)$ than in ^3P $(S=1)$ is due to the fact that there are more antiparallel spin pairs in ^1D than in ^3P. On the other hand, the reason why $|E^{corr}|$ is greater in ^1S $(L=0)$ than in ^1D $(L=2)$ is due to the fact that the two valence electrons are less likely to be on opposite sides of the nucleus in ^1S than in ^1D. The above fact is reasonable in the light of the interpretation of Hund's first and second rules.

To conclude, Hund's second rule is interpreted as follows: the two valence electrons in the larger L state are more likely to be on opposite sides of the nucleus, and hence nuclear screening is reduced. Therefore, the two electrons experience the nuclear charge more effectively to contract the valence electron density distribution toward the nucleus, leading to a greater V_{en} in the larger L state.

From the HF analysis of intracule and extracule densities, Koga *et al.* concluded that two electrons in the larger L state are more likely to be on opposite sides of the nucleus.[35] The present study supports their HF conclusion and at the same time demonstrates that correlation does not change the HF interpretation of Hund's rules.

From a comparison of inequalities (15) and (16), we have found that the decreasing order of V_{ee}^{corr} for the $3p$ atoms is opposite to the one for the $2p$ atoms. The reason may be considered as follows: the motion of electrons is correlated under the predominant influence of the nuclear attractive Coulomb field. The net value of V_{ee}^{corr} depends on two different correlation effects: (i) the avoiding motion of electrons that forms the so-called Coulomb hole (direct effect) and (ii) the correlation-induced contraction of the electron density distribution (indirect effect). Both of the two components of $V^{corr}(=V_{en}^{corr}+V_{ee}^{corr})$ are determined by a complicated interplay of V_{en}^{corr} and V_{ee}^{corr} under the condition $2T^{corr}+V_{en}^{corr}+V_{ee}^{corr}=0$. The indirect effect is enhanced as compared with the direct effect as Z is increased from the $2p$ atoms to the $3p$ atoms. This is the reason why the decreasing order of V_{ee}^{corr} is reversed for the $3p$ and $2p$ atoms.

From inequalities (15) and (16), we have arrived at the following conclusion common to the first and second rules: the greater $|E^{corr}|$ for the lower S or L state is ascribed to both the greater $|V_{ee}^{corr}|$ and $|V_{en}^{corr}|$ for the $2p$ atoms and to the greater $|V_{en}^{corr}|$ alone for the $3p$ atoms.

Inequality (16) is an unexpected result of the present study. However, these inequalities are a consequence of a complicated self-consistency between V_{en}^{corr}, V_{ee}^{corr}, and T^{corr} under the condition of $2T^{corr}+V_{en}^{corr}+V_{ee}^{corr}=0$. As an illustration, we mention an unexpected correlation effect for the $1s^22s2p$ excited configuration of the Be atom $(Z=4)$, which has already been reported by several authors. According to their CI calculations, $V_{ee}^{corr}<0$ holds for the ^3P term but unexpectedly $V_{ee}^{corr}>0$ for the ^1P term.[24,29] This means that correlation in rare cases of excited states can give rise to an increase in V_{ee} as compared with HF. Our preliminary MCHF calculation reconfirmed this fact.

The above unexpected correlation effect can be interpreted in a manner analogous to the interpretation of Hund's rules. Both the Coulomb hole and the Fermi hole have the effect of reducing the contribution of V_{ee} from short interelectronic distances. However, the presence of the two holes has also the effect of reducing the Hartree screening of the nucleus at short interelectronic distances. As a result, the electron density distribution contracts toward the nucleus. The exchange-induced reduction in screening increases the overall contribution of V_{ee} and overwhelms the reduction in V_{ee} due to the Fermi hole. Therefore, it is no wonder that an analogous increase in V_{ee} due to the Coulomb hole is observed for the rare cases of the excited states.

It is interesting to compare the correlation effect on V_{en} between atoms and molecules in the interpretation of Hund's rule. In the case of CH_2, it has been concluded by multireference CI (MRCI) that $|V_{en}^{corr}|$ is greater for the ground state $(^3B_1)$ than for the second excited state $(^1B_1)$, i.e., $V_{en}^{corr}(^3B_1) < V_{en}^{corr}(^1B_1) < 0$; the correlational virial ratio is accurate to three significant figures $(-V^{corr}/T^{corr}=1.999)$.[63] The reason

for the above inequality may be considered as follows. Unlike atoms, there are additional geometrical freedoms necessary to appropriately describe the difference in the molecular structure between two stationary states. The molecular geometry of the CH_2 ground state is formed in such a way that each valence electron can experience the nuclear charge Z more effectively as compared with the excited state. The inclusion of correlation also changes the molecular geometry for each of the $^3B_1$ and $^1B_1$ states. In order to make a correlation analysis based on the virial theorem in molecules, one has to evaluate energy components for each of two molecular geometries that is variationally determined with and without correlation.[64]

It is much more complicated to make a comparison of correlation effects on the Hund's spin-multiplicity rule in molecules than in atoms. This is because the simultaneous changes in the molecular geometry and in the spin-multiplicity give rise to additional differences in the correlational features between the two states.

D. Correlation effects on $D(r)$

The appropriate evaluation of V_{en}^{corr} is a challenging problem in computational quantum chemistry particularly for the second half of the $2p$ atoms (N ~ Ne). This is because of the small magnitude of V_{en}^{corr}. To evaluate V_{en}^{corr} quantitatively, it is necessary to give a sufficiently accurate description of a subtle correlation-induced change in the radial density distribution throughout the whole space. Otherwise, one cannot obtain any reliable value of V_{en}^{corr} with its correct sign.

The correlational virial theorem is one of the most powerful criteria for the evaluation of correlation effects. From the present MCHF calculations, it is concluded that the value of V_{en}^{corr} is negative for all the ground state of the He–Ca atoms (Z=2–20). This subsection is devoted to a detailed description of the correlation-induced change in the radial density distribution.

In Fig. 2, we make a comparison of the total radial density distribution $D(r)=4\pi r^2\rho(r)$ between HF (solid line) and MCHF (dashed line). Here, $\rho(r)$ is the spherically averaged electron density defined by Eq. (10). Figures 2(a) and 2(b) show $D(r)$ for the ground state (^3P term) of the carbon and silicon atoms as a representative of the $2p$ and $3p$ atoms, respectively. In the figures, each HF orbital contribution is also plotted to understand how the atomic shell structure (i.e., the K-, L-, and M-shell) is constructed from the components.

As can be seen from Fig. 2, the correlation-induced change in $D(r)$ is quite subtle. The most prominent correlation-induced change in $D(r)$ is seen around "the valence-shell," i.e., the L-shell region for the carbon atom and the M-shell region for the silicon atom. As has been mentioned in Sec. IV B, it is difficult to give a physical meaning to MCHF orbitals, in contrast to HF orbitals. However, as has been emphasized by Boyd, the concept of the shell structure survives even if correlation is included.[65] Hence, it is concluded that the correlation-induced change in $D(r)$ arises mainly from the valence-shell region.

Figure 3 shows the correlation-induced change in the

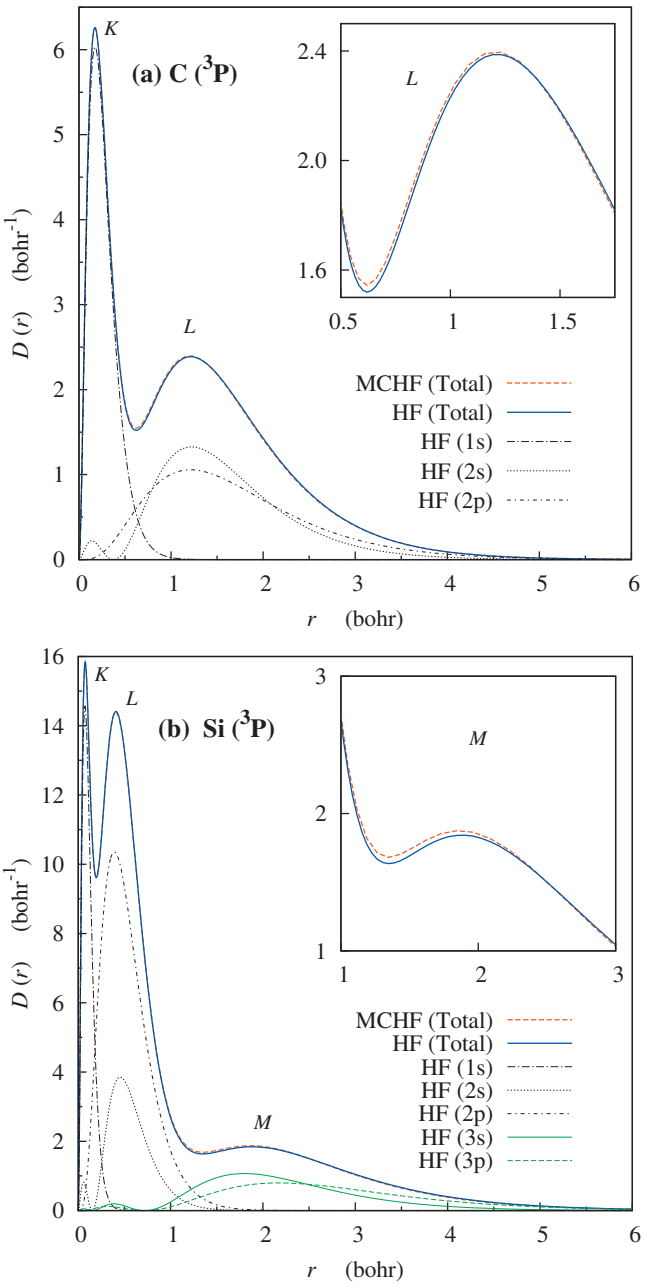

FIG. 2. Comparison of the total radial density distribution $D(r)\equiv 4\pi r^2\rho(r)$ between HF (—) and MCHF(SD,10m) (----) calculations for the ground state of the carbon and silicon atoms. Each HF orbital contribution is also plotted.

radial density distribution $D^{corr}(r)$ for each of the LS terms of the $2p$ (C, N, O) and $3p$ (Si, P, S) atoms. $D^{corr}(r)$ is defined as the difference in $D(r)$ between MCHF(SD,10m) and HF,

$$D^{corr}(r) = 4\pi r^2[\rho^{MCHF}(r) - \rho^{HF}(r)]. \quad (17)$$

So far as we know, this is the first report on an accurately evaluated $D^{corr}(r)$ for the excited LS terms of the $2p$ and $3p$ atoms, while Meyer *et al.*[66] reported similar results of $D^{corr}(r)$ for the ground LS terms of the Li–Ar atoms using MRCI. The integration of $D^{corr}(r)$ over the whole range of r, $[0,\infty]$ leads to zero because of the total electronic charge conservation,

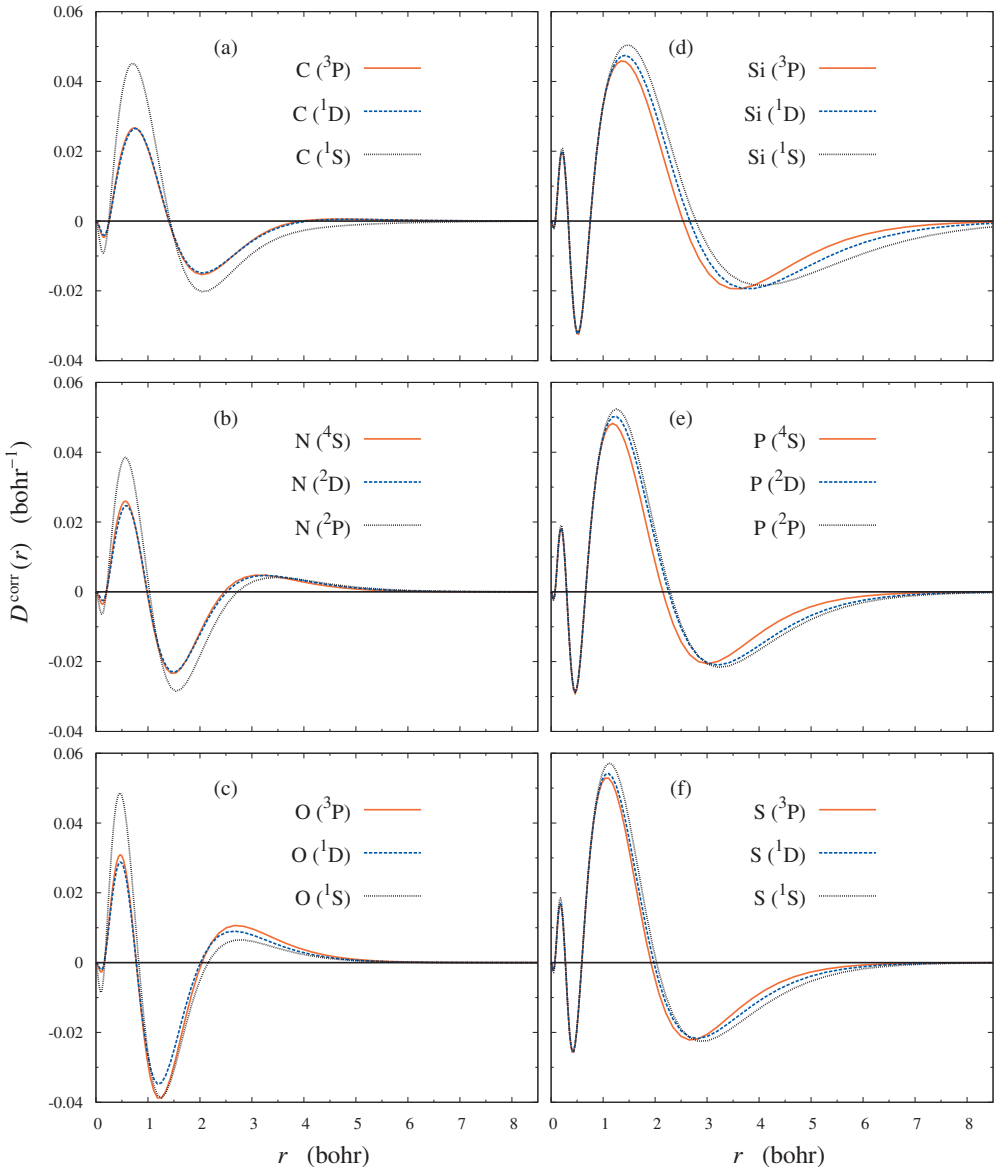

FIG. 3. Correlation-induced change in the radial density distribution $D^{corr}(r)$ for the $2p$ (C, N, O) and $3p$ (Si, P, S) atoms, defined as a difference between MCHF(SD,10m) and HF calculations.

$$\int_0^\infty D^{corr}(r)dr = 0. \tag{18}$$

The electron-nucleus attraction energy V_{en} is written as

$$V_{en} = -Z\langle r^{-1}\rangle = -Z\int_0^\infty r^{-1}D(r)dr, \tag{19}$$

and hence, V_{en}^{corr} is given as

$$V_{en}^{corr} = -Z\int_0^\infty r^{-1}D^{corr}(r)dr. \tag{20}$$

We have made a detailed analysis of $D^{corr}(r)$ over the whole range of distances from the nucleus. Correlation has the effect of reducing the Hartree–Fock screening of the nucleus at short interelectronic distances and $D(r)$ contracts toward the nucleus as a result. Aside from the complicated changes in $D^{corr}(r)$ observed in the immediate vicinity of the nucleus, the characteristic feature of $D^{corr}(r)$ common to the $2p$ and $3p$ atoms is that there appears a large positive peak on the small side of r and a large negative peak on the large side of r.

For the second half of the $2p$ atoms, an additional positive peak appears in the larger r region far from the nucleus and $D^{corr}(r)$ tends to zero from the positive side, accordingly. For the first half of the $2p$ atoms and all the $3p$ atoms, $D^{corr}(r)$ tends to zero from the negative side since there appears no such additional positive peak. The above-mentioned behaviors of $D^{corr}(r)$ as a function of r mean that

$$\int r^{-1}D^{corr}(r)dr > 0. \tag{21}$$

It is then concluded that $V_{en}^{corr} < 0$ for all the LS terms of the $2p$ and $3p$ atoms.

The magnitude of $E^{corr}(=-T^{corr}=V^{corr}/2)$ of the atoms increases monotonically with increasing Z, but the magni-

tude of its components, V_{en}^{corr} and V_{ee}^{corr}, does not show such a monotonic behavior. Here, we discuss such behavior of V_{en}^{corr} in terms of $D^{corr}(r)$.

For every *LS* term of the nitrogen and oxygen atoms, the electron density far from the nucleus is increased under the influence of the long-range correlation arising from a direct consequence of the electron-electron repulsive Coulomb interaction. A similar correlation effect has been observed for the ground state of the helium atom.[67] The small magnitude of V_{en}^{corr} for the second half of the $2p$ atoms is due to a large amount of cancellation among contributions of Eq. (21) from the short, intermediate, and long values of r. A very slight correlation-induced increase in the electron density far from the nucleus can also be observed for the ^3P and ^1D terms of the carbon atom, although the corresponding $D^{corr}(r)$ far from the nucleus is less than 10^{-4} bohr^{-1} in magnitude.

The reason why such a correlation-induced increase can be observed in the electron density $\rho(r)$ far from the nucleus is considered as follows: the asymptotic form of $\rho(r)$ far from the nucleus in an atom is analytically given as[68,69]

$$\rho(r) \sim \exp(-2\sqrt{2\mathrm{IE}}r), \tag{22}$$

where IE denotes the first ionization energy for an atom. According to Koopmans' theorem, the negative sign of the highest occupied-orbital energy $-\varepsilon_{max}$ in HF corresponds to the first ionization energy $\mathrm{IE_{KT}}$ in which correlation and relaxation effects are neglected. Hence, the following asymptotic form holds in the HF approximation:

$$\rho^{HF}(r) \sim \exp(-2\sqrt{2\mathrm{IE_{KT}}}r). \tag{23}$$

If Koopmans' theorem overestimates the ionization energy as compared with experiment ($\mathrm{IE_{KT}} > \mathrm{IE}$), then it follows from Eqs. (22) and (23) that $\rho^{HF}(r) < \rho(r)$ far from the nucleus. This inequality means that correlation increases the electron density $\rho(r)$ there. Actually, Koopmans' theorem overestimates the ionization energy by about 0.9–3.6 eV for the N–Ne atoms as compared with the experiment.[70] This is consistent with the fact that correlation increases $\rho(r)$ significantly far from the nucleus for the nitrogen and oxygen atoms, as shown in Fig. 3. We have also confirmed that the present MCHF can reproduce a similar correlation-induced increase in $\rho(r)$ for the fluorine and neon atoms. Meyer *et al.*[66] reported that MRCI also gives a similar result for the ground state of the N–Ne atoms.

$D^{corr}(r)$ in the region of about $r < 1$ bohr is indistinguishable between the three *LS* terms arising from the same electronic configuration of the $3p$ atoms. This region corresponds to *K*- and *L*-shell of the $3p$ atoms, as shown in Fig. 2(b). On the other hand, in the region of about $r > 1$ bohr corresponding to *M*-shell of the $3p$ atoms, a significant difference in $D^{corr}(r)$ is observed between the three *LS* terms. The reason for the above statement may be considered as follows: the *LS* symmetries of the atoms are essentially determined from the valence electronic configuration, and hence the contribution of $D^{corr}(r)$ from the core electrons is almost the same for the three *LS* terms.

"Atomic size" becomes smaller with increasing atomic number Z within the same row of the Periodic Table.[71] This is because the screening of the nucleus due to occupied orbitals becomes more and more incomplete with increasing Z until the halogen atoms. Then the complete screening of the nucleus is suddenly realized for the noble gas atoms. As the atomic size contracts with increasing Z, the positive and negative peak positions of $D^{corr}(r)$ gradually shift toward the nucleus in the order C, N, O (Z=6,7,8) and Si, P, S (Z=14,15,16).

A quite small negative peak of $D^{corr}(r)$ in the immediate vicinity of the nucleus is observed for all the $2p$ and $3p$ atoms. It may be concluded that the presence of the above negative peaks reflects a slight correlation-induced expansion of core orbitals.

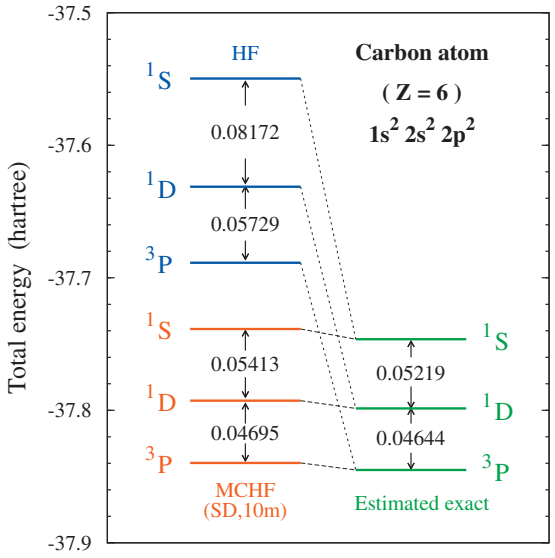

FIG. 4. Comparison of the energy level of the ^3P, ^1D, and ^1S terms arising from the $1s^2 2s^2 2p^2$ configuration of the carbon atom, obtained from three different methods, i.e., HF, MCHF(SD,10m), and estimated exact.

E. Correlation effects on the energy differences ΔE, ΔV_{en}, ΔV_{ee}, and ΔT between *LS* terms

In Fig. 4 we make a comparison of three different sets of energy levels for the ^3P, ^1D, and ^1S terms arising from the $1s^2 2s^2 2p^2$ configuration of the carbon atom (Z=6), which are obtained from HF, MCHF(SD,10m), and the estimated exact (see Sec. IV A). As can be seen from the figure, the three MCHF(SD,10m) energy levels are in quantitatively good agreement with the estimated exact result, with respect to both their absolute values $|E|$ and their differences $|\Delta E|$. MCHF(SD,10m) has successfully confirmed that the correlation-induced lowering in E is greater for the upper levels to reduce $|\Delta E|$. The above trend has also been observed for all the remaining $2p$ and $3p$ atoms.

Table VIII gives a list of numerical values of the total energy difference ΔE in the interpretation of Hund's first and second rules for the $2p$ and $3p$ atoms. In the table, a comparison is made between energy differences ΔE^{calc} calculated from HF and MCHF(SD,10m) and the most reliable experimental energy difference ΔE^{expt} obtained from the latest spectroscopy analysis.[58] The virial ratio for the energy difference $-\Delta V/\Delta T$ is also given in the last two column for HF and MCHF(SD,10m).

TABLE VIII. Energy difference $\Delta E(=\Delta T+\Delta V)$ and the ratio $-\Delta V/\Delta T$ obtained from HF and MCHF (SD,10m) calculations. Experimental energy difference ΔE (Expt.) is also listed. Error percentage (%) for HF and MCHF(SD,10m) in the evaluation of ΔE, which is defined as $\%\Delta E^{\text{error}}=[(\Delta E^{\text{calc}}-\Delta E^{\text{expt}})/\Delta E^{\text{expt}}]\times 100$ is also given in parentheses. All energies are in hartree units.

	ΔE ($\%\Delta E^{\text{error}}$)					$-\Delta V/\Delta T$	
Hund's first rule	HF		MCHF(SD,10m)		Expt.[a]	HF	MCHF(SD,10m)
$C(^3P)-C(^1D)$	−0.057 29	(23.4%)	−0.046 95	(1.1%)	−0.046 44	2.000 002 7	2.000 000 4
$N(^4S)-N(^2D)$	−0.104 76	(19.6%)	−0.088 89	(1.5%)	−0.087 59	2.000 000 0	1.999 999 4
$O(^3P)-O(^1D)$	−0.080 13	(10.8%)	−0.072 28	(−0.03%)	−0.072 30	2.000 001 9	2.000 000 7
$Si(^3P)-Si(^1D)$	−0.039 15	(36.4%)	−0.031 60	(10.1%)	−0.028 70	1.999 996 7	2.000 003 9
$P(^4S)-P(^2D)$	−0.069 91	(35.1%)	−0.056 95	(10.0%)	−0.051 76	1.999 997 7	1.999 999 9
$S(^3P)-S(^1D)$	−0.052 54	(24.8%)	−0.044 07	(4.7%)	−0.042 09	2.000 015 4	2.000 027 4
	ΔE ($\%\Delta E^{\text{error}}$)					$-\Delta V/\Delta T$	
Hund's second rule	HF		MCHF(SD,10m)		Expt.[a]	HF	MCHF(SD,10m)
$C(^1D)-C(^1S)$	−0.081 72	(56.6%)	−0.054 13	(3.7%)	−0.052 19	1.999 997 7	1.999 998 3
$N(^2D)-N(^2P)$	−0.068 07	(55.4%)	−0.045 47	(3.8%)	−0.043 81	2.000 001 8	1.999 998 7
$O(^1D)-O(^1S)$	−0.118 24	(44.8%)	−0.082 96	(1.6%)	−0.081 67	1.999 998 7	1.999 999 1
$Si(^1D)-Si(^1S)$	−0.056 12	(35.4%)	−0.046 88	(13.1%)	−0.041 44	2.000 001 6	1.999 998 7
$P(^2D)-P(^2P)$	−0.045 57	(35.8%)	−0.038 12	(13.6%)	−0.033 54	2.000 003 6	2.000 012 2
$S(^1D)-S(^1S)$	−0.077 67	(31.7%)	−0.065 11	(10.4%)	−0.058 97	2.000 012 1	2.000 014 8

[a]NIST Atomic Spectra Database (Ref. 58).

For convenience, we have introduced the following error percentage in order to give a systematic comparison between ΔE^{expt} and ΔE^{calc} for the $2p$ and $3p$ atoms:

$$\%\Delta E^{\text{error}}=\frac{\Delta E^{\text{calc}}-\Delta E^{\text{expt}}}{\Delta E^{\text{expt}}}\times 100, \tag{24}$$

where ΔE^{calc} denotes the total energy difference calculated from HF (ΔE^{HF}) or MCHF (ΔE^{MCHF}). The smaller value of $\%\Delta E^{\text{error}}$ means better agreement with the experiment.

As can be seen from the value of $\%\Delta E^{\text{error}}$, HF systematically overestimates $|\Delta E|$ compared to the experiment in its interpretation of Hund's first and second rules. For a good agreement with ΔE^{expt}, it is necessary to evaluate correlation with a sufficiently high recovering percentage of the correlation energy for each of the two stationary states being compared. MCHF improves the HF overestimates of $|\Delta E|$ to give excellent agreement with the experiment owing to due account of correlation. HF overestimates $|\Delta E|$ more seriously for the second rule than for the first rule. In other words, correlation plays a more important role in the interpretation of the second rule.

The SDTQ-CI calculation for the carbon atom by Sasaki and Yoshimine is in rather better agreement with ΔE^{expt} than the present MCHF(SD,10m) calculation. Their SDTQ-CI energy differences (and the corresponding error percentages) are $E(^3P)-E(^1D)=-0.0469$ ($\%\Delta E^{\text{error}}=0.99$) for the first rule and $E(^1D)-E(^1S)=-0.0539$ ($\%\Delta E^{\text{error}}=3.26$) for the second rule. However, they have not reported each of the energy components V_{en}, V_{ee}, T, as well as the virial ratio $-V/T$. They also have not calculated the excited LS terms of the B–Ne atoms except for the carbon atom.

In the following, we give a detailed discussion about the difference in E, V_{en}, V_{ee}, and T between the two LS terms being compared in order to give a detailed interpretation of how correlation improves the HF overestimate of $|\Delta E|$ by changing its components ΔV_{en}, ΔV_{ee}, and ΔT. For this purpose, it is necessary to satisfy the virial ratio for the energy difference $-\Delta V/\Delta T=2$ with high accuracy in both HF and MCHF. In other words, it is necessary to satisfy with high accuracy *the virial ratio for the difference in correlation energy* $-\Delta V^{\text{corr}}/\Delta T^{\text{corr}}=2$, where $\Delta T^{\text{corr}}\equiv\Delta T^{\text{MCHF}}-\Delta T^{\text{HF}}$ and $\Delta V^{\text{corr}}\equiv\Delta V^{\text{MCHF}}-\Delta V^{\text{HF}}$.

As is shown in Table VIII, the virial ratio for the energy difference $-\Delta V/\Delta T=2$ is accurate to five to seven significant figures for the $2p$ atoms and four to seven significant figures for the $3p$ atoms in both HF and MCHF(SD,10m). Accordingly, $-\Delta V^{\text{corr}}/\Delta T^{\text{corr}}=2$ is accurate to four to six significant figures for the $2p$ and $3p$ atoms. This accuracy is sufficient to arrive at a unified interpretation of Hund's first and second rules and a correct understanding of how correlation improves the HF overestimate of $|\Delta E|$ through its components ΔV_{en}, ΔV_{ee}, and ΔT.

Generally, the convergence of $-V/T=2$ is slower for the $3p$ atoms than for the $2p$ atoms. Furthermore, $|\Delta E|$ is smaller for the $3p$ atoms than for the $2p$ atoms. For example, if one compares the $3p$ and $2p$ atoms in the same group, the ratio $|\Delta E^{\text{expt}}(2p)|/|\Delta E^{\text{expt}}(3p)|$ is 1.62–1.72 for the first rule and 1.26–1.39 for the second rule. Therefore, it is more difficult to satisfy $-\Delta V/\Delta T=2$ with high accuracy for the $3p$ atoms than for the $2p$ atoms. The smaller $|\Delta E|$ in the $3p$ atoms is due to the fact that a greater amount of cancellation occurs between ΔV_{en} and ΔV_{ee}.

Figure 5 gives a systematic comparison of the energy differences between the different LS terms of the $2p$ and $3p$ atoms,

$$\begin{aligned}\Delta E &\equiv E(LS)-E(L'S'),\\ \Delta V_{\text{en}} &\equiv V_{\text{en}}(LS)-V_{\text{en}}(L'S'),\\ \Delta V_{\text{ee}} &\equiv V_{\text{ee}}(LS)-V_{\text{ee}}(L'S'),\end{aligned} \tag{25}$$

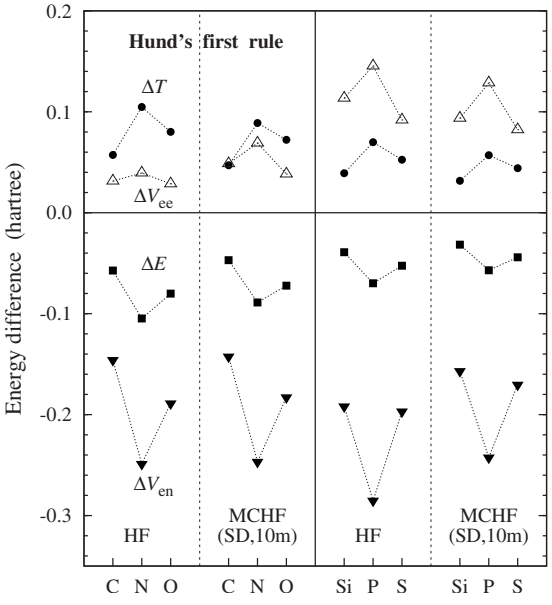

FIG. 5. Comparison of the energy differences ΔE (■), ΔV_{en} (▼), ΔV_{ee} (△), and ΔT (●) between the ground and the first excited *LS* terms (i.e., between ^3P and ^1D for the C, O, Si, and S atoms and between ^4S and ^2D for the N and P atoms) in the interpretation of Hund's first rule, calculated from HF and MCHF(SD,10m).

$$\Delta T \equiv T(LS) - T(L'S')$$

in the interpretation of the first rule by HF and MCHF. Here, each of the energy differences in Eq. (25) is defined such that $E(LS) < E(L'S') < 0$; the *LS* term is more stable than the $L'S'$ term. Figure 6 gives a similar comparison in the interpretation of the second rule. From the virial relation, $\Delta E = (\Delta V_{en} + \Delta V_{ee})/2$ for atoms, it follows $|\Delta V_{en} - \Delta E| = |\Delta V_{ee} - \Delta E|$. Hence, the position of ΔE is exactly located in the middle point between ΔV_{en} and ΔV_{ee}. The relation $\Delta T = -\Delta E$ holds between any two stationary states of atoms, molecules, and solids. In practice, these simple but exact relations are not easy to satisfy with high accuracy in the variational calculations. Note that these relations are satisfied with high accuracy in Figs. 5 and 6.

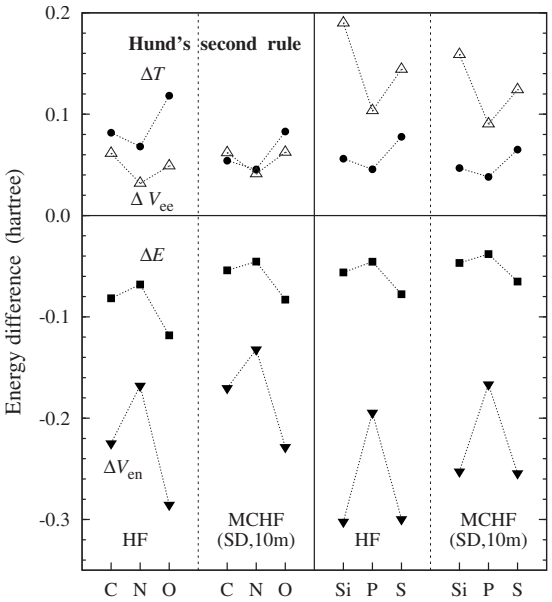

FIG. 6. Comparison of the energy differences ΔE (■), ΔV_{en} (▼), ΔV_{ee} (△), and ΔT (●) between the first and the second excited *LS* terms, (i.e., between ^1D and ^1S for the C, O, Si, and S atoms and between ^2D and ^2P for the N and P atoms) in the interpretation of Hund's second rule, calculated from HF and MCHF(SD,10m).

As is obvious from Figs. 5 and 6, the negative value of ΔE is a direct consequence of the negative value of ΔV_{en}. It is demonstrated in the two figures that the correct interpretation of both Hund's first and second rules involves an increase in V_{ee}, i.e., a positive value of ΔV_{ee} for all the $2p$ and $3p$ atoms.

Katriel and Pauncz proved that $-1 < \Delta V_{ee}/\Delta V_{en} < 1$, based on the scaling arguments within the single-configuration approximation.[6,7] The ratio $\Delta V_{ee}/\Delta V_{en}$ is negative ($\Delta V_{ee} > 0$ and $\Delta V_{en} < 0$) for neutral atoms and isoelectronic anions. Interestingly, the ratio $\Delta V_{ee}/\Delta V_{en}$ for isoelectronic cations turns to be positive ($\Delta V_{ee} < 0$ and $\Delta V_{en} < 0$) if the nuclear charge Z exceeds a certain critical value. This is because ΔV_{ee} turns to be negative, although ΔV_{en} remains negative and predominant. The above change in the sign of ΔV_{ee} common to the two rules is ascribed to the fact that under the stronger influence of the nucleus charge a decrease in the electron-electron repulsion between the valence orbitals themselves becomes greater in magnitude than an increase in the electron-electron repulsion between the valence and core orbitals. In the limit $Z \to \infty$, $\Delta V_{ee}/\Delta V_{en}$ approaches 1 but never exceeds 1 ($\Delta V_{en} \lessapprox \Delta E \lessapprox \Delta V_{ee} < 0$). Even for the extremely positive-charged cations Hund's first and second rules are ascribed to a greater V_{en} in the more stable *LS* terms. V_{ee} plays a minor role in the stabilization of any stationary state.

As is obvious from Figs. 5 and 6, the correlation-induced reduction of $|\Delta E|$ in the interpretation of the two rules for the $2p$ atoms is ascribed to a combination of the reduction in $|\Delta V_{en}|$ and increase in $|\Delta V_{ee}|$. On the other hand, the correlation-induced reduction of $|\Delta E|$ for the $3p$ atoms is mostly ascribed to the reduction in $|\Delta V_{en}|$ alone. As is evident from the virial theorem, the reduction in $|\Delta E|$ is always accompanied by a reduction in $|\Delta T| \left(= \frac{1}{2}|\Delta V|\right)$.

F. Correlation effects on $\Delta D(r)$

In Fig. 7 we have given a systematic comparison of the difference in the total radial density distribution for the $2p$ and $3p$ atoms,

$$\Delta D(r) \equiv 4\pi r^2 [\rho(LS;r) - \rho(L'S';r)] \tag{26}$$

in the interpretation of Hund's first and second rules. The solid and dashed lines denote $\Delta D(r)$ in HF and MCHF, respectively. So far as we know, a systematic comparison of $\Delta D(r)$ between MCHF and HF has not been reported for these $2p$ and $3p$ atoms, which is needed to investigate how correlation affects $\Delta D(r)$. In Eq. (26), $\Delta D(r)$ is defined such that $E(LS) < E(L'S') < 0$ in the same way as ΔE. Here, the integration of $\Delta D(r)$ over the whole range of r, $[0,\infty]$ leads to zero because of the overall electronic charge conservation.

As can be seen from Fig. 7, the total radial density distribution contracts toward the nucleus in the more stable *LS* terms. $\Delta D(r) > 0$ for the small r region and $\Delta D(r) < 0$ for the

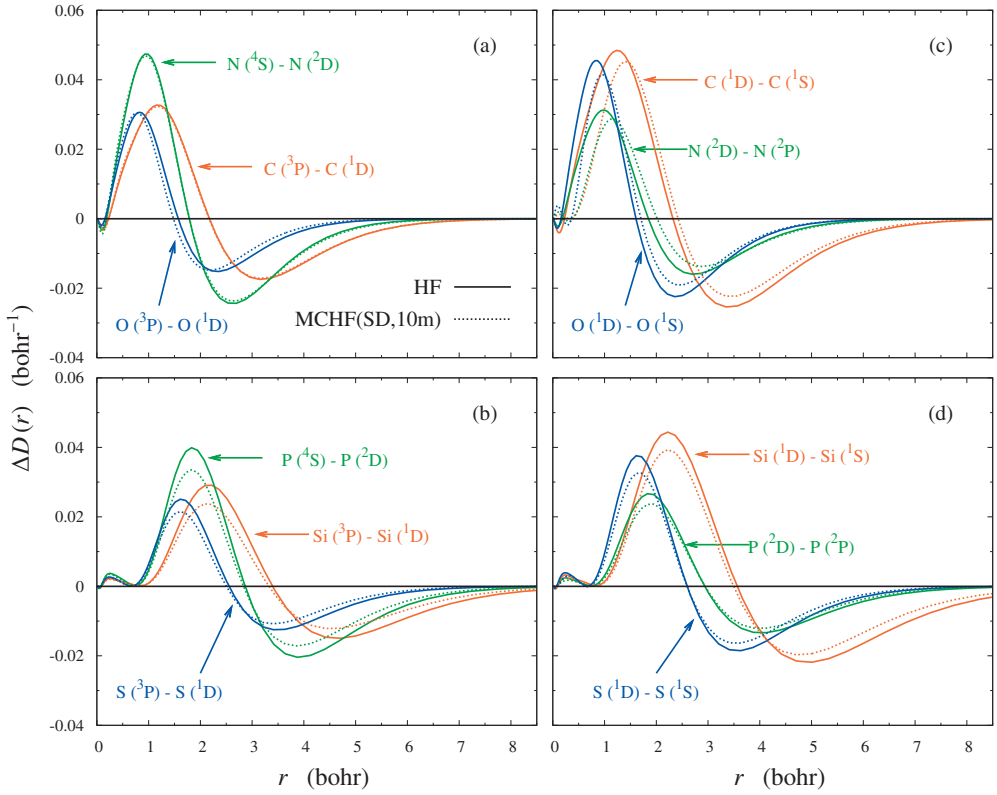

FIG. 7. Difference in the radial density distribution, i.e., $\Delta D(r)$ in the interpretation of Hund's first and second rules, obtained from HF (—) and MCHF(SD,10m) (----).

large r region. Both Hund's first and second rules are a direct consequence of the above contraction of $D(r)$ due to the reduced screening in the more stable LS terms. The characteristic features of $\Delta D(r)$ are common to HF and MCHF except for a shift in peak positions and a change in their amplitudes; correlation does not qualitatively change $\Delta D(r)$.

As for the interpretation of the first rule, the amplitude of the positive and negative peaks of $\Delta D(r)$ are both largest for the nitrogen atom of the $2p$ atoms and for the phosphorus atom of the $3p$ atoms. On the other hand, as for the second rule, similar positive and negative peaks of $\Delta D(r)$ are smallest in magnitude for the nitrogen and phosphorus atoms.

Let us consider the physical reason for the above difference between the two rules. First, we focus our attention on the effect of the total spin-angular momentum S. The three valence electrons in the ^4S term of the N and P atoms can "feel" the nuclear charge Z more effectively owing to the largest value of $S=3/2$. In other words, there is a more effective exchange-induced reduction in screening in the ^4S term of the N and P atoms. As a result of the greater contraction, the magnitude of $\Delta D(r)$ is greater for the N and P atoms in the interpretation of the first rule.

Next, we focus our attention on the effect of the total orbital-angular momentum L. In the interpretation of the second rule, $\Delta D(r)$ between $L=2$ and $L=0$ (i.e., $^1D-^1S$ of the C, O, Si, and S atoms) is larger than $\Delta D(r)$ between $L=2$ and $L=1$ (i.e., $^2D-^2P$ of the N and P atoms) in magnitude. In other words, the larger/smaller difference in L gives rise to the larger/smaller difference in $\Delta D(r)$. Hence, $\Delta D(r)$ is smallest in magnitude for the N and P atoms in the interpretation of the second rule.

Note that the above argument of the L dependence in the second rule persists even for the first rule if one makes a similar analysis of the L dependence as well as the S dependence. In the interpretation of the first rule, $\Delta D(r)$ between $L=0$ and $L=2$ (i.e., $^4S-^2D$ of the N and P atoms) is larger than $\Delta D(r)$ between $L=1$ and $L=2$ (i.e., $^3P-^1D$ of the C, O, Si, and S atoms) in magnitude. As a result of the above combined effects of S and L, $\Delta D(r)$ is largest in magnitude for the N and P atoms in the interpretation of the first rule.

In Figs. 5 and 6, ΔE, ΔT, ΔV_{en}, and ΔV_{ee} plotted with respect to Z for C, N, O ($Z=6,7,8$) and Si, P, S ($Z=14,15,16$) take a "V-shaped" or "Λ-shaped" form. The relation of the V- or Λ-shaped form is reversed between the interpretation of the Hund's first and second rules. The amplitude of the positive and negative peaks of $\Delta D(r)$ discussed above is responsible for the V- or Λ-shaped form of the energy differences. A greater ΔE is a direct consequence of a greater ΔV_{en} that is caused by the greater contraction of the electron density distribution, i.e., a greater $\Delta D(r)$.

From a comparison of MCHF and HF, it is concluded that correlation reduces the magnitude of $\Delta D(r)$ for the $2p$ and $3p$ atoms in the interpretation of the first and second rules. This is consistent with the fact that the correlation-induced reduction in $|\Delta E|$ involves a reduction in $|\Delta V_{en}|$.

We shall close this subsection by discussing similarities and differences between the exchange and correlation effects on the total radial density distribution $D(r)$. A similarity in the two effects is the reduced screening, i.e., exchange and correlation both give rise to a reduction in the Hartree screening of the nucleus at short interelectronic distances to contract $D(r)$ toward the nucleus.

A difference in the two effects is observed between $\Delta D(r)$ and $D^{\mathrm{corr}}(r)$ in the large r region. $\Delta D(r)$ for the first rule tends to zero in the limit $r \to \infty$ from the negative side for all the $2p$ and $3p$ atoms considered. As for $D^{\mathrm{corr}}(r)$, correlation gives rise to a significant increase in the electron density far from the nucleus for the second half of the $2p$ atoms because of long-range correlation due to the direct Coulomb repulsion, which is in contrast to the essentially short-range nature of exchange due to the Pauli exclusion principle.

The short-range nature of exchange has already been discussed through a detailed analysis of the pair distribution function for the low-lying excited states of the helium atom by Katriel–Pauncz[6,7] and Boyd–Coulson[30] and through a systematic analysis of the electron-pair intracule density for group 14–16 atoms in the Periodic Table (including the C, N, O, Si, P, and S atoms) by Koga *et al.*[35]

V. DISCUSSION

In the interpretation of Hund's first and second rules for the $3d$ atoms, we encounter a difficulty that has not been seen for the $2p$ and $3p$ atoms. One of the remarkable differences between the $3d$ atoms and the $2p$ and $3p$ atoms lies in the experimental fact that the first and second rules do not necessarily hold between the excited LS terms arising from the ground configuration of the $3d$ atoms.

So far as we make a comparison between the ground and the excited LS terms arising from the ground configuration of the $3d$ atoms, we are confident that the stabilization mechanism of the ground term of the $3d$ atoms can be interpreted in the same way as the forementioned unified interpretation of the first and second rules for the $2p$ and $3p$ atoms. In most cases, HF correctly reproduces the experimental order of energy levels of the LS terms; in a small number of cases, the inclusion of correlation beyond HF is necessary. In the framework of HF, it is concluded for all cases of the ground configuration and for almost all cases of excited configurations that the lower E of the LS terms is ascribed to the greater V_{en} that is gained at the cost of increasing V_{ee}.[36]

We are confident that the predominant role of V_{en} in the realization of the lowest V in the ground state is valid for the ground term arising from the ground configuration of the $2p$, $3p$, and $3d$ atoms even if correlation is included. The electron-electron repulsion energy V_{ee} is subject to the electron-nucleus attraction energy V_{en} not only for the $2p$ and $3p$ atoms but also for the $3d$ atoms and hence both V_{en} and V_{ee} attain to the largest values in magnitude.

VI. CONCLUDING REMARKS

The virial theorem is a necessary condition for the formation of stationary states. It means the uniqueness of how a lower stationary state is stabilized relative to a higher state. Those variational theories that satisfy the Pauli exclusion principle under the condition of the virial theorem are indispensable for the correct and unified interpretation of Hund's first and second rules. Both HF and MCHF are suitable for this purpose.

We have demonstrated that both Hund's first and second rules are due to a greater electron-nucleus attraction energy that is a consequence of the reduced screening. The Hartree screening of the nucleus is reduced at short interelectronic distances, and hence the valence electrons feel the nuclear charge more effectively to give rise to the contraction of the valence orbitals. The reduced screening is realized through different mechanisms between the first and the second rules. The mechanism for the first rule is due to a greater number of Fermi hole contributions in the highest spin-multiplicity state. The mechanism for the second rule is due to the fact that two electrons are more likely to be on opposite sides of the nucleus in the highest total orbital-angular momentum state.

Penetration of the valence orbitals into the immediate vicinity of the nucleus gives rise to an extra screening so as to give a slight but significant expansion of the core orbitals. A combination of contraction of the valence orbitals and expansion of the core orbitals, which is observed in the interpretation of Hund's first and second rules, gives rise to an increase in the overall contributions of V_{ee}, overwhelming a reduction in the short interelectronic contribution of V_{ee} in the more stable state.

ACKNOWLEDGMENTS

The authors are grateful to Dr. Mark A. Watson for his fruitful comments and Dr. Soh Ishii and Dr. Hannes Raebiger for their valuable discussions. The authors wish to express their gratitude to the referees for pointing out several pertinent issues about the traditional interpretation of Hund's rules and suggesting some changes to make the manuscript more readable and clearer. One of the authors (T.O.) would like to express his appreciation to Professor Hirohiko Kono and Professor Tsuyoshi Kato for their encouragement. This work has been supported by the Grant-in-Aid for Japan Society for the Promotion of Science (JSPS) research fellows (Grant No. 20·6432). K.H. is grateful for a JSPS Postdoctoral Fellowship for Research Abroad. The computation in this work has been performed using SR11000 supercomputer and the facilities of the Center for Computational Materials Science of the Institute for Materials Research, Tohoku University.

[1] K. Hongo, R. Maezono, Y. Kawazoe, H. Yasuhara, M. D. Towler, and R. J. Needs, J. Chem. Phys. **121**, 7144 (2004).
[2] T. Oyamada, K. Hongo, Y. Kawazoe, and H. Yasuhara, J. Chem. Phys. **125**, 014101 (2006).
[3] K. Hongo, T. Oyamada, Y. Maruyama, Y. Kawazoe, and H. Yasuhara, J. Magn. Magn. Mater. **310**, e560 (2007).
[4] K. Hongo, T. Oyamada, Y. Maruyama, Y. Kawazoe, and H. Yasuhara, Mater. Trans. **48**, 662 (2007).
[5] F. L. Pilar, *Elementary Quantum Chemistry*, 2nd ed. (McGraw-Hill, New York, 1990).
[6] J. Katriel, Theor. Chim. Acta **23**, 309 (1972); **26**, 163 (1972).
[7] J. Katriel and R. Pauncz, Adv. Quantum Chem. **10**, 143 (1977).
[8] F. Hund, Z. Phys. **33**, 345 (1925); **34**, 296 (1925); *Linienspektren und periodisches System der Elemente* (Springer-Verlag OHG, Berlin, 1927).
[9] J. C. Slater, Phys. Rev. **34**, 1293 (1929); *Quantum Theory of Matter*, 1st ed. (McGraw-Hill, 1951); *Quantum Theory of Atomic Structure* (McGraw-Hill, New York, 1960), Vol. I.
[10] I. N. Levine, *Quantum Chemistry*, 6th ed. (Prentice-Hall, New Jersey, 2008).
[11] S. Huzinaga, *The Molecular Orbital Method* (Iwanami Shoten, Tokyo,

1980) (in Japanese).
[12] J. P. Dahl, *Introduction to the Quantum World of Atoms and Molecules* (World Scientific, Singapore, 2001).
[13] J. Killingbeck, J. Phys. C **3**, 23 (1970).
[14] The proof of the virial theorem for the first-order perturbation theory in Ref. 13 is based on the assumption that the unperturbed system has no degeneracies.
[15] B. Schiff, H. Lifson, C. L. Pekeris, and P. Rabinowitz, Phys. Rev. **140**, A1104 (1965).
[16] Y. Accad, C. L. Pekeris, and B. Schiff, Phys. Rev. A **4**, 516 (1971).
[17] J. P. Colpa and M. F. J. Islip, Mol. Phys. **25**, 701 (1973).
[18] E. R. Davidson, J. Chem. Phys. **41**, 656 (1964); **42**, 4199 (1965).
[19] R. P. Messmer and F. W. Birss, J. Phys. Chem. **73**, 2085 (1969).
[20] R. L. Snow and J. L. Bills, J. Phys. Chem. **78**, 1334 (1974).
[21] It has been pointed out in Ref. 20 that column I of Table I in Ref. 19 reports incorrect numerical results. If the calculations were performed correctly, the ^3P state would have a higher V_{ee} than the ^1P state even when each of the $1s$ and $2p$ orbitals were approximated by one Slater-type function, as shown in Ref. 20.
[22] A. Lemberger and R. Pauncz, Acta Phys. Acad. Sci. Hung. **27**, 169 (1969).
[23] J. Killingbeck, Mol. Phys. **25**, 455 (1973).
[24] H. Tatewaki and K. Tanaka, J. Chem. Phys. **60**, 601 (1974).
[25] J. P. Colpa, A. J. Thakkar, V. H. Smith, Jr., and P. Randle, Mol. Phys. **29**, 1861 (1975).
[26] N. Moiseyev, J. Katriel, and R. J. Boyd, J. Phys. B **8**, L130 (1975).
[27] E. Clementi and C. Roetti, At. Data Nucl. Data Tables **14**, 177 (1974).
[28] S. Fraga, J. Karwouski, and K. M. S. Saxena, *Handbook of Atomic Data* (Elsevier, Amsterdam, 1976).
[29] I. Shim and J. P. Dahl, Theor. Chim. Acta **48**, 165 (1978).
[30] R. J. Boyd and C. A. Coulson, J. Phys. B **6**, 782 (1973); **7**, 1805 (1974).
[31] R. J. Boyd, Theor. Chim. Acta **33**, 79 (1974).
[32] R. J. Boyd, Nature (London) **310**, 480 (1984).
[33] T. Koga and H. Matsuyama, J. Phys. B **31**, 3765 (1998).
[34] T. Koga, H. Matsuyama, J. M. Molina, and J. S. Dehesa, Eur. Phys. J. D **7**, 17 (1999).
[35] T. Koga, H. Matsuyama, J. S. Dehesa, and A. J. Thakkar, J. Chem. Phys. **110**, 5763 (1999).
[36] T. Koga and Y. Koshida, J. Chem. Phys. **111**, 54 (1999).
[37] Y. Sajeev, M. Sindelka, and N. Moiseyev, J. Chem. Phys. **128**, 061101 (2008).
[38] T. Sako, J. Paldus and G. H. F. Diercksen, Phys. Rev. A **81**, 022501 (2010).
[39] D. R. Hartree and W. Hartree, Proc. R. Soc. London, Ser. A **154**, 588 (1936).
[40] C. Froese Fischer, *The Hartree-Fock Method for Atoms—A Numerical Approach* (Wiley, New York, 1977).
[41] C. Froese Fischer, T. Brage, and P. Jönsson, *Computational Atomic Structure. An MCHF Approach* (Institute of Physics, Bristol, 1997).
[42] C. Froese Fischer, in *Springer Handbook of Atomic, Molecular, and Optical Physics*, 2nd ed. edited by Gordon W. F. Drake, ed. (Springer, 2007), Chap. 21, pp. 307–323.
[43] G. Marc and W. G. McMillan, in *Advances in Chemical Physics*, edited by I. Prigogine and S. A. Rice (Wiley, New York, 1985), Vol. 58, pp. 209–361.
[44] C. Froese Fischer, Comput. Phys. Rep. **3**, 273 (1986).
[45] C. Froese Fischer, Comput. Phys. Commun. **64**, 369 (1991); **64**, 399 (1991); **64**, 431 (1991).
[46] D. R. Hartree, *The Calculation of Atomic Structures* (Wiley, New York, 1957).
[47] C. Froese Fischer, Comput. Phys. Commun. **43**, 355 (1987).
[48] G. Gaigalas and C. Froese Fischer, Comput. Phys. Commun. **98**, 255 (1996).
[49] C. Froese Fischer, Can. J. Phys. **51**, 1238 (1973).
[50] C. Froese Fischer, Comput. Phys. Commun. **128**, 635 (2000).
[51] A. Hibbert and C. Froese Fischer, Comput. Phys. Commun. **64**, 417 (1991).
[52] L. Sturesson and C. Froese Fischer, Comput. Phys. Commun. **74**, 432 (1993).
[53] C. Froese Fischer, G. Tachiev, G. Gaigalas, and M. R. Godefroid, Comput. Phys. Commun. **176**, 559 (2007).
[54] A. Borgoo, O. Scharf, G. Gaigalas, and M. Godefroid, Comput. Phys. Commun. **181**, 426 (2010).
[55] In the comparison of the two $\rho(r)$, we have enhanced the significant figures of mixing coefficients c_i to avoid arithmetic errors arising from numerical data of the original ATSP2K code.
[56] E. R. Davidson, S. A. Hagstrom, S. J. Chakravorty, V. Mesier Umar, and C. Froese Fischer, Phys. Rev. A **44**, 7071 (1991).
[57] S. J. Chakravorty, S. R. Gwaltney, E. R. Davidson, F. A. Parpia, and C. Froese Fischer, Phys. Rev. A **47**, 3649 (1993).
[58] Yu. Ralchenko, F.-C. Jou, D. E. Kelleher, A. E. Kramida, A. Musgrove, J. Reader, W. L. Wiese, and K. Olsen, (2007). NIST Atomic Spectra Database (version 3.1.2) (online), available: http://physics.nist.gov/asd3 [June 2, 2007], National Institute of Standards and Technology, Gaithersburg, MD.
[59] E. Buendía, F. J. Gálvez, P. Maldonado, and A. Sarsa, J. Chem. Phys. **131**, 044115 (2009).
[60] F. Sasaki and M. Yoshimine, Phys. Rev. A **9**, 17 (1974).
[61] See supplementary material at http://dx.doi.org/10.1063/1.3488099 for the decomposition of V_{en} and V_{ee} (Tables S1 and S2) and the convergence of E, V, T, and $-V/T$ (Table S3).
[62] C. Froese Fischer, J. Comput. Phys. **13**, 502 (1973).
[63] Y. Maruyama, K. Hongo, M. Tachikawa, Y. Kawazoe, and H. Yasuhara, Int. J. Quantum Chem. **108**, 731 (2008).
[64] K. Hongo, Y. Kawazoe, and H. Yasuhara, Int. J. Quantum Chem. **107**, 1459 (2007).
[65] R. J. Boyd, J. Phys. B **9**, L69 (1976).
[66] H. Meyer, T. Müller, and A. Schweig, J. Mol. Struct.: THEOCHEM **360**, 55 (1996).
[67] C. J. Umrigar and X. Gonze, Phys. Rev. A **50**, 3827 (1994).
[68] M. M. Morrell, R. G. Parr, and M. Levy, J. Chem. Phys. **62**, 549 (1975).
[69] J. Katriel and E. R. Davidson, Proc. Natl. Acad. Sci. U.S.A. **77**, 4403 (1980).
[70] K. Hongo, Y. Kawazoe, and H. Yasuhara, Mater. Trans. **47**, 2612 (2006).
[71] J. Mason, J. Chem. Educ. **65**, 17 (1988).

Supplementary material to the article in The Journal of Chemical Physics: Unified interpretation of Hund's first and second rules for $2p$ and $3p$ atoms

Takayuki Oyamada[1], Kenta Hongo[2], Yoshiyuki Kawazoe[3], and Hiroshi Yasuhara[3]

1. Department of Chemistry, Graduate School of Science,
Tohoku University, 6-3 Aoba, Aramaki, Aoba-ku, Sendai 980-8578, Japan
2. Department of Chemistry and Chemical Biology,
Harvard University, 12 Oxford Street, Cambridge, MA 02138, USA
3. Institute for Materials Research, Tohoku University, 2-1-1 Katahira, Aoba-ku, Sendai 980-8577, Japan

(Dated: April 21, 2010)

As supplementary material, we give here two tables which we think is helpful for the unified interpretation of Hund's first and second rules. We also show in the third table how we have attained the accurate fulfillment of the virial theorem in the present MCHF calculations.

TABLE S1: Decomposition of V_{en} into its orbital contributions $V_{\mathrm{en}}^{(nl)}$ for the LS terms of (a) the carbon and (b) the silicon atoms in HF. The differences of $V_{\mathrm{en}}^{(nl)}$ between the ^3P and ^1D terms and between the ^1D and ^1S terms, i.e., $\Delta V_{\mathrm{en}}^{(nl)}$ are shown in the last two columns. The last row is the total sum of each column. In the first column, the number of electron in the nl-orbital N_{nl} is also shown in parentheses.

(a) Carbon atom ($Z = 6$) $1s^2 2s^2 2p^2$

Orbital	C (^3P)	C (^1D)	C (^1S)	$^3P - {}^1D$	$^1D - {}^1S$
1s (2)	-67.97327	-67.97936	-67.98813	+0.00609	+0.00877
2s (2)	-10.76158	-10.81158	-10.88926	+0.05000	+0.07768
2p (2)	-9.40204	-9.20003	-8.88880	−0.20201	−0.31123
V_{en} (Total)	-88.13688	-87.99097	-87.76619	−0.14592	−0.22478

(b) Silicon atom ($Z = 14$) $[1s^2 2s^2 2p^6] 3s^2 3p^2$

Orbital	Si (^3P)	Si (^1D)	Si (^1S)	$^3P - {}^1D$	$^1D - {}^1S$
1s (2)	-380.27220	-380.27307	-380.27434	+0.00087	+0.00127
2s (2)	-72.53124	-72.53622	-72.54359	+0.00498	+0.00737
2p (6)	-206.33609	-206.32756	-206.31821	−0.00853	−0.00935
3s (2)	-16.89046	-16.94089	-17.02245	+0.05043	+0.08156
3p (2)	-13.38488	-13.14531	-12.76226	−0.23957	−0.38306
V_{en} (Total)	-689.41486	-689.22304	-688.92084	−0.19182	−0.30220

TABLE S2: Decomposition of $V_{\rm ee}$ into its orbital-pair contributions $V_{\rm ee}^{(nl-n'l')}$ for the LS terms of (a) the carbon and (b) the silicon atoms in HF. The differences of $V_{\rm ee}^{(nl-n'l')}$ between the ^3P and ^1D terms and between the ^1D and ^1S terms, i.e., $\Delta V_{\rm ee}^{(nl-n'l')}$ are shown in the last two column. The last row is the total sum of each column. In the first column, the number of the orbital pair $N_{\rm pair}$ is also shown in parentheses.

(a) Carbon atom ($Z = 6$) $1s^2 2s^2 2p^2$

Orbital-pair	C (^3P)	C (^1D)	C (^1S)	$^3P - {}^1D$	$^1D - {}^1S$
1s-1s (1)	3.50910	3.50953	3.51015	−0.00043	−0.00062
2s-1s (4)	3.13959	3.15189	3.17098	−0.01230	−0.01909
2s-2s (1)	0.57288	0.57540	0.57933	−0.00252	−0.00393
2p-1s (4)	3.06046	2.99581	2.89600	+0.06464	+0.09982
2p-2s (4)	1.98767	1.96333	1.92381	+0.02434	+0.03952
2p-2p (1)	0.48994	0.53234	0.58669	−0.04240	−0.05435
$V_{\rm ee}$ (Total)	12.75965	12.72831	12.66697	+0.03134	+0.06134

(b) Silicon atom ($Z = 14$) $[1s^2 2s^2 2p^6] 3s^2 3p^2$

Orbital-pair	Si (^3P)	Si (^1D)	Si (^1S)	$^3P - {}^1D$	$^1D - {}^1S$
1s-1s (1)	8.44255	8.44257	8.44261	−0.00003	−0.00004
2s-1s (4)	8.72679	8.72729	8.72803	−0.00050	−0.00074
2s-2s (1)	1.61053	1.61064	1.61080	−0.00011	−0.00016
2p-1s (12)	28.34223	28.34107	28.33981	+0.00115	+0.00127
2p-2s (12)	17.84077	17.84082	17.84109	−0.00005	−0.00027
2p-2p (15)	24.79893	24.79720	24.79523	+0.00173	+0.00197
3s-1s (4)	2.30760	2.31401	2.32440	−0.00642	−0.01038
3s-2s (4)	2.12565	2.13076	2.13905	−0.00511	−0.00828
3s-2p (12)	6.48917	6.50514	6.53107	−0.01597	−0.02593
3s-3s (1)	0.40999	0.41110	0.41292	−0.00111	−0.00182
3p-1s (4)	1.89588	1.86207	1.80801	+0.03380	+0.05406
3p-2s (4)	1.77980	1.74907	1.69982	+0.03073	+0.04925
3p-2p (12)	5.34265	5.25032	5.10236	+0.09233	+0.14796
3p-3s (4)	1.29709	1.28231	1.25781	+0.01478	+0.02450
3p-3p (1)	0.29653	0.32825	0.36968	−0.03172	−0.04143
$V_{\rm ee}$ (Total)	111.70614	111.59263	111.40267	+0.11351	+0.18996

TABLE S3: Convergence of E, V, T, and $-V/T$ with respect to iteration in a MCHF(SD,8k) calculation for the ground state (^3P) of the carbon atom. Generally, an improvement in E with respect to each iteration, though rather small, leads to a significant improvement in the fulfillment of $-V/T = 2$. This is because the convergence of T and V is slower than that of $E(= T + V)$.

Iteration	E	V	T	$-V/T$
10	-37.838814218	-75.6770696	37.8382554	2.000015
20	-37.838883642	-75.6775998	37.8387161	2.0000044
30	-37.838887833	-75.6777342	37.8388464	2.0000011
40	-37.838888233	-75.6777576	37.8388694	2.00000050
50	-37.838888385	-75.6777665	37.8388781	2.00000027
60	-37.838888442	-75.6777711	37.8388827	2.00000015
70	-37.838888464	-75.6777736	37.8388851	2.000000088
80	-37.838888474	-75.6777749	37.8388864	2.000000054
90	-37.838888480	-75.6777755	37.8388870	2.000000038
100	-37.838888485	-75.6777757	37.8388872	2.000000034
120	-37.838888491	-75.6777757	37.8388872	2.000000034
140	-37.838888496	-75.6777756	37.8388871	2.000000038
160	-37.838888499	-75.6777754	37.8388869	2.000000041
180	-37.838888501	-75.6777755	37.8388870	2.000000041
200	-37.838888502	-75.6777756	37.8388871	2.000000036
220	-37.838888503	-75.6777758	37.8388873	2.000000032
240	-37.838888504	-75.6777757	37.8388872	2.000000033
260	-37.838888504	-75.6777758	37.8388873	2.000000031
280	-37.838888505	-75.6777760	37.8388875	2.000000028
300	-37.838888505	-75.6777761	37.8388876	2.000000024
350	-37.838888505	-75.6777764	37.8388879	2.000000016
400	-37.838888505	-75.6777765	37.8388880	2.000000013
450	-37.838888506	-75.6777766	37.8388881	2.000000010
500	-37.838888506	-75.6777768	37.8388883	2.0000000048
550	-37.838888506	-75.6777769	37.8388884	2.0000000025
600	-37.838888506	-75.6777771	37.8388886	1.9999999982
620	-37.838888506	-75.6777770	37.8388885	1.9999999994